PHYSICAL REVIEW A VOLUME 20, NUMBER 5 NOVEMBER 1979

Echoes in gaseous media: A generalized theory of rephasing phenomena

T. W. Mossberg, R. Kachru, and S. R. Hartmann
Columbia Radiation Laboratory, Department of Physics, Columbia University, New York, New York 10027

A. M. Flusberg
Avco Everett Research Corporation, Everett, Massachusetts 02149

(Received 26 March 1979)

The primary objective of this paper is to provide a formalism to predict and characterize the echoes which may be produced in a gaseous sample by an arbitrary sequence of one- or two-frequency laser excitation pulses which successively transfer atomic population between two or more atomic energy levels. The resulting echoes can occur at times which depend on the relative frequencies of the excitation pulses as well as on the times at which the pulses were applied. Using an idealized model of the excitation pulses and the atoms, the authors derive a simple transformation equation which provides the density matrix of a single atom after a general excitation sequence. Equations are derived which utilize the single-atom density matrix to predict the properties of the echoes (if any) which result. The means by which the sample of atoms "remembers" the information necessary to produce different types of echoes is discussed, and it is then shown how a study of the echo can provide information concerning the atomic relaxation processes which tend to destroy this information. It is observed that trilevel echoes can be used to determine the relaxation characteristics of superposition states between energy levels coupled by two-photon transitions. In the case of certain other echoes (such as the three-excitation-pulse stimulated echo) the authors discuss the heretofore unappreciated fact that the sample remembers the "echo information" via a nonthermal velocity distribution of the atoms in *one specific atomic state*. In these cases a study of the echo behavior can provide information pertaining to the relaxation processes affecting only the one atomic state. The formalism developed is used to predict the properties of several echo effects. First, to provide a connection with previous work, the well-known photon echo is briefly discussed. Then important new properties of the three-excitation-pulse-stimulated echo are described. Finally, three different types of trilevel echo are analyzed. Each of the trilevel echoes discussed has widespread applicability in the study of relaxation processes.

INTRODUCTION

It has recently been demonstrated[1] that experimental techniques utilizing the trilevel echo[2] can be used to great advantage to make relaxation measurements over a wide range of superposition states. In particular, in atomic Na vapor the noble-gas-induced relaxation properties of the $3\,^2S_{1/2}$-$n\,^2S_{1/2}$ and $3\,^2S_{1/2}$-$n\,^2D_{3/2}$ superposition states have been studied, with the principal quantum number n of the upper level ranging from 4 to $\gtrsim 40$. The ease with which the various trilevel echo techniques can be applied and the wide range of states to which they are applicable ensures that the trilevel echo effect will find extensive use in the field of coherent transient studies in atomic and molecular physics. In this paper we present a theoretical treatment of echo effects in a Doppler-broadened gaseous medium which facilitates the analysis and understanding of such *new echo effects* as the trilevel echo, as well as providing basic new insight into such older effects as the three-excitation-pulse stimulated echo.[3]

Unlike the well-known echo effects produced in two-level spin[3] and electronic systems,[4-6] trilevel echoes[1,2] (and related effects in spin systems[7]) cannot in general be completely described in terms of the usual vector model[8,9] or its generalizations.[10,11] Attempts have been made in the past to provide alternative means of describing echo formation, but only specific excitation sequences have been considered.[12] We attempt here to present a treatment sufficiently general to describe the echo effects (if any) to be expected after an arbitrary sequence of travelling-wave excitation pulses in a Doppler-broadened gaseous sample of multilevel atoms. The formalism presented can be used to describe not only trilevel echoes (and the two-level echoes as special cases) but also effects such as the Raman echo[13,14] and the two-photon echo.[15] When applied to the three-excitation-pulse two-level (stimulated) echo, interesting new insights into the effect are obtained.[16]

The plan of the paper is as follows: In Sec. I a formalism is developed to provide the single-atom density matrix after an arbitrary sequence of model excitation pulses. Section II discusses the conditions under which echoes will arise in a large-compared-to-the-emission-wavelength Doppler-broadened sample of atoms, and how the results of Sec. I can be used to determine when these conditions are satisfied. Section III briefly discus-

ses the echo decay which results from atomic relaxation. Finally, Sec. IV provides a series of detailed examples of the analysis of certain echo effects.

I. SINGLE-ATOM THEORY

A. Introduction and definitions

The objective of Sec. I is to provide a simple method for determining the state of a particular multilevel atom after excitation by a series of one- or two-frequency pulses of electromagnetic radiation. For simplicity we assume throughout this section that only three levels of the atom are coupled by the excitation fields; however, in Sec. IV C the treatment will be generalized to describe an excitation sequence which couples four levels.

Figure 1 defines the types of three-level atom discussed here. The nondegenerate levels $|0\rangle$, $|1\rangle$, and $|2\rangle$ have energies $\hbar\Omega_0 = 0$, $\hbar\Omega_1$, and $\hbar\Omega_2$. The interference effects which arise when the levels consist of a number of degenerate or nearly degenerate sublevels are ignored. These echo–quantum-beat effects[17,18] are interesting, but generally do not change the basic nature of the results.

Considering the electric dipole operator p to be a scalar, we define

$$p_{ij} = \langle i|p|j\rangle \tag{1.1a}$$

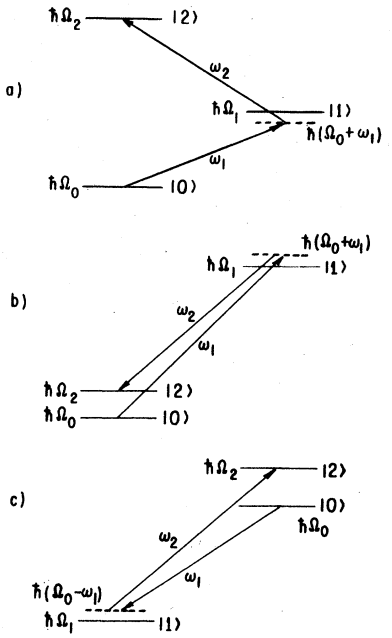

FIG. 1. Different level arrangements discussed in this paper are shown. In each case the $|2\rangle$-$|0\rangle$ transition is forbidden. Generally we assume that the population is initially in the state of lowest energy.

and assume

$$p_{20} = 0\,. \tag{1.1b}$$

Consider a moving atom whose instantaneous center-of-mass position is $\vec{r}$, which we assume may be treated classically. The electric field it sees is given in scalar form by

$$E(\vec{r},t) = E_1(\vec{r},t) + E_2(\vec{r},t)\,, \tag{1.2a}$$

where t is the time and

$$E_n \equiv \mathcal{E}_n \exp[-i(\omega_n t - \vec{k}_n\cdot\vec{r})] + \text{c.c.} \quad (n=1,2)\,. \tag{1.2b}$$

It is assumed that the fields of Eqs. (1.2) are plane-wave Fourier-transform-limited square pulses, i.e., that $\mathcal{E}_n$ is constant throughout the duration of the pulse. The near-resonance condition

$$|\Omega_1 - \omega_1| \ll |\Omega_1 - \omega_2|\,, \tag{1.3a}$$

$$|(\Omega_2 - \Omega_1) - \omega_2| \ll |(\Omega_2 - \Omega_1) - \omega_1| \tag{1.3b}$$

is imposed on the two components of E. This allows us to assume that the E_1 (E_2) component of E interacts only with the $|1\rangle$-$|0\rangle$ ($|2\rangle$-$|1\rangle$) transition and simplifies the calculations. We also impose the following two-photon-resonance condition on the excitation fields: It is required that either

$$|\omega_1 + \omega_2| = |\Omega_2 - \Omega_0| \tag{1.4a}$$

or

$$|\omega_1 - \omega_2| = |\Omega_2 - \Omega_0|\,, \tag{1.4b}$$

depending on the level configuration of the atoms.

The time evolution of the atom is determined by the Schrödinger equation

$$\frac{d\psi(t)}{dt} = -i\hbar^{-1}(H_0 + V)\psi(t)\,, \tag{1.5}$$

where H_0 is the Hamiltonian for the unperturbed three-level atom and V represents the atom-excitation field interaction. Our method of solving Eq. (1.5) follows the work of Hartmann[13]; however, many other useful approaches have been presented.[19] The basis vectors of the matrices represented in Eq. (1.5) are chosen to be the time-independent eigenstates of H_0, i.e.,

$$H_0 = \begin{pmatrix} \langle 0|H_0|0\rangle & \langle 0|H_0|1\rangle & \langle 0|H_0|2\rangle \\ \langle 1|H_0|0\rangle & \langle 1|H_0|1\rangle & \langle 1|H_0|2\rangle \\ \langle 2|H_0|0\rangle & \langle 2|H_0|1\rangle & \langle 2|H_0|2\rangle \end{pmatrix} \tag{1.6a}$$

$$= \begin{pmatrix} 0 & 0 & 0 \\ 0 & \hbar\Omega_1 & 0 \\ 0 & 0 & \hbar\Omega_2 \end{pmatrix}. \tag{1.6b}$$

In the electric dipole approximation the interaction is given by $V = -pE$. Thus

$$V=\begin{pmatrix} 0 & -p_{01}\{\mathcal{E}_1^* \exp[i(\omega_1 t-\vec{k}_1\cdot\vec{r})]+\text{c.c.}\} & 0 \\ -p_{10}\{\mathcal{E}_1 \exp[-i(\omega_1 t-\vec{k}_1\cdot\vec{r})]+\text{c.c.}\} & 0 & -p_{12}\{\mathcal{E}_2^* \exp[i(\omega_2 t-\vec{k}_2\cdot\vec{r})]+\text{c.c.}\} \\ 0 & -p_{21}\{\mathcal{E}_2 \exp[-i(\omega_2 t-\vec{k}_2\cdot\vec{r})]+\text{c.c.}\} & 0 \end{pmatrix}. \tag{1.7}$$

B. Solution of the single-atom equations of motion

Eq. (1.5) may be transformed into a Schrödinger-type equation whose Hamiltonian is, to a certain approximation, independent of time, and which we can therefore solve exactly. Using this result, we solve for the state of the atom after an *arbitrary sequence* of one- or two-frequency traveling-wave excitation pulses.

We define an interaction-picture wave function ψ_ω given by

$$\psi_\omega(t)=\exp(iAt)\psi(t), \tag{1.8}$$

where for the atoms shown in Fig. 1 of types "a," "b," and "c," respectively,

$$A=\begin{pmatrix} 0 & 0 & 0 \\ 0 & \omega_1 & 0 \\ 0 & 0 & \omega_1+\omega_2 \end{pmatrix}, \tag{1.9a}$$

$$A=\begin{pmatrix} 0 & 0 & 0 \\ 0 & \omega_1 & 0 \\ 0 & 0 & \omega_1-\omega_2 \end{pmatrix}, \tag{1.9b}$$

$$A=\begin{pmatrix} 0 & 0 & 0 \\ 0 & -\omega_1 & 0 \\ 0 & 0 & \omega_2-\omega_1 \end{pmatrix}. \tag{1.9c}$$

The wave function ψ_ω then satisfies

$$\frac{d\psi_\omega(t)}{dt}=-i\hbar^{-1}H_\omega\psi_\omega(t), \tag{1.10}$$

where

$$H_\omega=\exp(iAt)(H_0+V-A)\exp(-iAt). \tag{1.11}$$

Using the rotating-wave approximation,[9] one obtains

$$H_\omega=\begin{pmatrix} 0 & a^* & 0 \\ a & \Delta & b^* \\ 0 & b & 0 \end{pmatrix}, \tag{1.12}$$

where for type "a" atoms

$$a=-p_{10}\mathcal{E}_1\exp(i\vec{k}_1\cdot\vec{r}), \tag{1.13a}$$

$$b=-p_{21}\mathcal{E}_2\exp(i\vec{k}_2\cdot\vec{r}), \tag{1.13b}$$

$$\Delta=\hbar(\Omega_1-\omega_1); \tag{1.13c}$$

for type "b" atoms

$$a=-p_{10}\mathcal{E}_1\exp(i\vec{k}_1\cdot\vec{r}), \tag{1.14a}$$

$$b=-p_{12}\mathcal{E}_2^*\exp(-i\vec{k}_2\cdot\vec{r}), \tag{1.14b}$$

$$\Delta=\hbar(\Omega_1-\omega_1); \tag{1.14c}$$

and for type "c" atoms

$$a=-p_{01}\mathcal{E}_1^*\exp(-i\vec{k}_1\cdot\vec{r}), \tag{1.15a}$$

$$b=-p_{21}\mathcal{E}_2\exp(i\vec{k}_1\cdot\vec{r}), \tag{1.15b}$$

$$\Delta=\hbar(\Omega_1+\omega_1). \tag{1.15c}$$

The quantities a and b carry all the information pertaining to the relative phase of the electric dipole moment(s) of the atom. Hence they are referred to as "phase factors." The complex conjugates of a and b, while also referred to as phase factors, will occasionally be referred to specifically as "conjugate phase factors." The magnitude of the phase factor a (b) is proportional to the Rabi flipping frequency associated with resonant single-frequency excitation of the $|1\rangle$-$|0\rangle$ ($|2\rangle$-$|1\rangle$) transition. Products of a phase factor and its conjugate such as aa^* and bb^*, which appear often below, carry no phase information.

We now assume that the optical pulse is so short that the vector $\vec{r}$, which denotes the instantaneous position of the atom, may be considered a constant over the pulse duration. This assumption is equivalent to ignoring inhomogeneous (Doppler) broadening *during* the pulse. It follows that H_ω is independent of time. We emphasize that this assumption is not crucial to the production of echoes; it is violated in most echo experiments done to date. However, treating $\vec{r}$ as a constant during the pulse greatly simplifies the theoretical analysis of echoes and does not change the fundamental results.[20]

Since H_ω is independent of t, Eq. (1.10) can be integrated to give an expression for the wave function after an excitation pulse

$$\psi_\omega(t)=M\psi_\omega(t_0), \tag{1.16}$$

where

$$M = \exp(-i\hbar^{-1}H_\omega t)\,. \tag{1.17}$$

The corresponding interaction-picture density matrix[21] $\rho_\omega(t) = \exp(iAt)\rho(t)\exp(-iAt)$ where $\rho(t)$ is the laboratory-frame density matrix, is given by

$$\rho_\omega(t) = M\rho_\omega(t_0)M^{-1}\,. \tag{1.18}$$

For an arbitrary sequence of j one- or two-frequency excitation pulses

$$\rho_\omega(t_f) = M_j M_{j-1}\cdots M_1\rho_\omega(t_i)t_0 M_1^{-1}\cdots M_{j-1}^{-1}M_j^{-1}\,, \tag{1.19}$$

where $\rho_\omega(t_0)$ and $\rho_\omega(t_f)$, respectively, represent the initial and final density matrix.

Consider now the explicit evaluation of the M matrix associated with a particular pulse. Since H_ω is not diagonal, explicit expressions for M are obtained from

$$M = S^{-1}\exp(-i\hbar^{-1}SH_\omega S^{-1}\tau)S\,, \tag{1.20}$$

where τ is the temporal width of the excitation pulse and S is the matrix which diagonalizes H_ω. We find that

$$S = \begin{pmatrix} -b/a^* & 0 & 1 \\ a/\lambda_+ & 1 & b^*/\lambda_+ \\ a/\lambda_- & 1 & b^*/\lambda_- \end{pmatrix}, \tag{1.21}$$

with

$$\lambda_\pm = \tfrac{1}{2}\{\Delta \pm [\Delta^2 + 4(bb^* + aa^*)]^{1/2}\}\,. \tag{1.22}$$

Then, using Eq. (1.20), we find M to be given by

$$\begin{pmatrix} \dfrac{-bb^*\varkappa - aa^*(\lambda_- e^{-i\theta_+/2} - \lambda_+ e^{-i\theta_-/2})}{\lambda_-\lambda_+\varkappa} & \dfrac{-a^*}{\varkappa}(e^{-i\theta_+/2} - e^{-i\theta_-/2}) & \dfrac{a^*b^*}{\lambda_-\lambda_+\varkappa}(\varkappa - \lambda_- e^{-i\theta_+/2} + \lambda_+ e^{-i\theta_-/2}) \\ \dfrac{-a}{\varkappa}(e^{-i\theta_+/2} - e^{-i\theta_-/2}) & \dfrac{1}{\varkappa}(\lambda_- e^{-i\theta_-/2} - \lambda_+ e^{-i\theta_+/2}) & \dfrac{-b^*}{\varkappa}(e^{-i\theta_+/2} - e^{-i\theta_-/2}) \\ \dfrac{ab}{\lambda_-\lambda_+\varkappa}(\varkappa - \lambda_- e^{-i\theta_+/2} + \lambda_+ e^{-i\theta_-/2}) & \dfrac{-b}{\varkappa}(e^{-i\theta_+/2} - e^{-i\theta_-/2}) & \dfrac{-aa^*\varkappa - bb^*(\lambda_- e^{-i\theta_+/2} - \lambda_+ e^{-i\theta_-/2})}{\lambda_-\lambda_+\varkappa} \end{pmatrix}, \tag{1.23}$$

where

$$\varkappa \equiv (\lambda_- - \lambda_+) \tag{1.24}$$

and

$$\theta_\pm \equiv 2\lambda_\pm\tau/\hbar\,. \tag{1.25}$$

The matrix M^{-1} is obtained from the expression for M by changing the signs of θ_+ and θ_-. It is understood that the value $\vec{r}$ which enters a particular M matrix through Eqs. (1.13)–(1.15) is the atomic position during the particular corresponding pulse. Since the position of an atom changes with time, Eq. (1.19) includes the effect of atomic motion *between* excitation pulses.

Although many echoes can be produced with non-intermediate-state resonant two-photon excitation and require the general M matrix for their complete description, the essential features of echo formation are more easily elucidated with a simpler M matrix. Thus restricting ourselves to resonant excitation, i.e., $\Delta = 0$, M becomes

$$M_R = \begin{pmatrix} \dfrac{bb^* + aa^*\cos\frac{1}{2}\theta}{aa^* + bb^*} & \dfrac{-ia^*\sin\frac{1}{2}\theta}{(aa^* + bb^*)^{1/2}} & \dfrac{-a^*b^*[1 - \cos\frac{1}{2}\theta]}{aa^* + bb^*} \\ \dfrac{-ia\sin\frac{1}{2}\theta}{(aa^* + bb^*)^{1/2}} & \cos(\tfrac{1}{2}\theta) & \dfrac{-ib^*\sin\frac{1}{2}\theta}{(aa^* + bb^*)^{1/2}} \\ \dfrac{-ab[1 - \cos\frac{1}{2}\theta]}{aa^* + bb^*} & \dfrac{-ib\sin\frac{1}{2}\theta}{(aa^* + bb^*)^{1/2}} & \dfrac{aa^* + bb^*\cos\frac{1}{2}\theta}{aa^* + bb^*} \end{pmatrix}, \tag{1.26}$$

where

$$\theta = 2(aa^* + bb^*)^{1/2}\tau/\hbar = (\theta_a^2 + \theta_b^2)^{1/2} \tag{1.27}$$

and $\theta_a = 2(aa^*)^{1/2}\tau/\hbar$ [$\theta_b = 2(bb^*)^{1/2}\tau/\hbar$] represents the area of the ω_1 (ω_2) component of the two-frequency pulse when it interacts with the $|1\rangle$-$|0\rangle$ ($|2\rangle$-$|1\rangle$) transition in the absence of the other frequency component. Used with Eqs. (1.18) and (1.19), the M (or M_R) matrix permits us to calculate the density matrix of an atom after interaction with the excitation pulses. Equations (1.18), (1.19), (1.23), and (1.26) thus represent the principal results of Sec. I.

Summarizing the highlights of Secs. IA and IB, we have taken the following model of the interaction of atoms with a series of one- or two-fre-

quency pulses: (i) The atoms are three-level systems. (ii) Level pair 0-1 (1-2) is coupled by frequency component ω_1 (ω_2) only. (iii) The center-of-mass position of each atom is considered a classically well-defined quantity. (iv) Each pulse is a temporally square plane wave which is so short that the individual atoms may be considered stationary *during* the pulse, but atomic center-of-mass motion *between* pulses is (implicitly) taken into account. Using this model and the rotating-wave approximation, we have derived a matrix which gives the exact state of each atom after an arbitrary sequence of pulses.

C. Calculation of the single-atom density matrix after different excitation sequences

As an application of the M_R matrix we consider the effect of a two-frequency pulse [Fig. 2(a)] on a type-a (Fig. 1) three-level atom initially in state $|0\rangle$. We have

$$\rho(t_0)=\begin{pmatrix}1&0&0\\0&0&0\\0&0&0\end{pmatrix}. \tag{1.28}$$

The interaction-picture density matrix $\rho_\omega(t_0)$ is in this case identical to $\rho(t_0)$. Thus substituting Eqs. (1.26) and (1.28) into Eq. (1.18), we find that after the excitation pulse

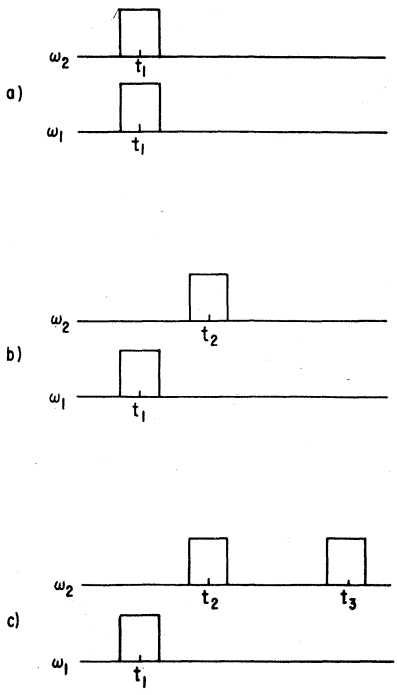

FIG. 2. Various excitation sequences considered in Sec. I. (a) Depicts a single two-frequency pulse. (b) Depicts two successive single-frequency pulses. (c) Same as (b) except that a second excitation pulse resonant with the $|2\rangle$-$|1\rangle$ transition is applied.

$$\rho_\omega(t_f)=\begin{bmatrix}\left(\frac{bb^*+aa^*\cos\frac{1}{2}\theta}{aa^*+bb^*}\right)^2 & \frac{ia^*\sin\frac{1}{2}\theta(bb^*+aa^*\cos\frac{1}{2}\theta)}{(aa^*+bb^*)^{3/2}} & \frac{-a^*b^*(1-\cos\frac{1}{2}\theta)(bb^*+aa^*\cos\frac{1}{2}\theta)}{(aa^*+bb^*)^2}\\ \frac{-ia\sin\frac{1}{2}\theta(bb^*+aa^*\cos\frac{1}{2}\theta)}{(aa^*+bb^*)^{3/2}} & \frac{aa^*\sin^2\frac{1}{2}\theta}{aa^*+bb^*} & \frac{iaa^*b^*\sin\frac{1}{2}\theta(1-\cos\frac{1}{2}\theta)}{(aa^*+bb^*)^{3/2}}\\ \frac{-ab(1-\cos\frac{1}{2}\theta)(bb^*+aa^*\cos\frac{1}{2}\theta)}{(aa^*+bb^*)^2} & \frac{-iaa^*b\sin\frac{1}{2}\theta(1-\cos\frac{1}{2}\theta)}{(aa^*+bb^*)^{3/2}} & \frac{aa^*bb^*(1-\cos\frac{1}{2}\theta)^2}{(aa^*+bb^*)^2}\end{bmatrix}. \tag{1.29}$$

If we set $b=b^*=0$, $\rho_\omega(t_f)$ in Eq. (1.29) should reduce to the familiar result for a two-level system. Indeed, we find

$$\rho_\omega(t_f)_{b=0}=\frac{1}{2}\begin{bmatrix}1+\cos\theta & ia^*(\sin\theta)/|a| & 0\\ -ia(\sin\theta)/|a| & 1-\cos\theta & 0\\ 0 & 0 & 0\end{bmatrix}. \tag{1.30}$$

Note that when a phase factor appears on the diagonal of Eq. (1.29) it is always multiplied by its conjugate phase factor, hence no phase information is present in the diagonal matrix elements. This is expected, since the diagonal elements of $\rho_\omega(t_f)$ refer to the population in the three levels; however, in the off-diagonal elements the single phase factors retain their phase information. Given the definitions of the phase factors, Eqs. (1.13)–(1.15), this implies that the relative phase of each off-diagonal element (and the associated electric dipole moment) is determined by the relative phase of the excitation field at $\vec{r}$, the location of the atom during excitation. Thus the relative phase of the oscillating electric dipole moments of different atoms will depend on the spatial separations of the atoms at the time of excitation.

We now consider [(see Fig. 2(b)] the application of two successive single-frequency excitation pulses of frequencies ω_1 and ω_2, respectively. In accordance with Eq. (1.19), M_R is applied twice—first with $b \equiv 0$, then with $a \equiv 0$. Using Eqs. (1.26) and (1.28) in Eq. (1.19), we find that after the second excitation pulse

$$\rho_\omega(t_f) = \begin{bmatrix} \cos^2\tfrac{1}{2}\theta_1 & \dfrac{ia^*\sin\theta_1\cos\tfrac{1}{2}\theta_2}{2|a|} & \dfrac{-a^*b^*\sin\theta_1\sin\tfrac{1}{2}\theta_2}{2|a||b|} \\ \dfrac{-ia\sin\theta_1\cos\tfrac{1}{2}\theta_2}{2|a|} & \sin^2\tfrac{1}{2}\theta_1\cos^2\tfrac{1}{2}\theta_2 & \dfrac{ib^*\sin^2\tfrac{1}{2}\theta_1\sin\theta_2}{2|b|} \\ \dfrac{-ab\sin\theta_1\sin\tfrac{1}{2}\theta_2}{2|a||b|} & \dfrac{-ib\sin^2\tfrac{1}{2}\theta_1\sin\theta_2}{2|b|} & \sin^2\tfrac{1}{2}\theta_1\sin^2\tfrac{1}{2}\theta_2 \end{bmatrix}, \tag{1.31}$$

where θ_i is the area of the ith pulse.

As in Sec. IB, it is understood here that the atomic position $\vec{r}$, which enters ρ_ω through Eqs. (1.13)–(1.15), may be different for the two pulses. We note that Eq. (1.31) has a considerably simpler appearance than Eq. (1.29). This is a characteristic difference between "two-photon" [(Eq. (1.29)] and "stepwise" [(Eq. (1.31)] excitation. In the two-photon case each frequency component of the excitation pulse affects the population in all three levels. The second pulse in the stepwise case affects only levels $|1\rangle$ and $|2\rangle$.

The three-pulse excitation scheme of Fig. 2(c) is important for calculations made below. Furthermore, it provides insight into several effects important in the production of echoes. Starting from Eq. (1.31) as the initial density matrix and using Eqs. (1.18) and (1.26), we find that after this excitation sequence

$$(\rho_\omega)_{00} = \cos^2\tfrac{1}{2}\theta_1\,, \tag{1.32a}$$

$$(\rho_\omega)_{11} = \sin^2\tfrac{1}{2}\theta_1[\cos^2\tfrac{1}{2}\theta_2\cos^2\tfrac{1}{2}\theta_3 + \sin^2\tfrac{1}{2}\theta_2\sin^2\tfrac{1}{2}\theta_3] - [\sin^2\tfrac{1}{2}\theta_1\sin\theta_2\sin\theta_3(b\beta^* + b^*\beta)]/4|b||\beta|\,, \tag{1.32b}$$

$$(\rho_\omega)_{22} = \sin^2\tfrac{1}{2}\theta_2[\cos^2\tfrac{1}{2}\theta_2\sin^2\tfrac{1}{2}\theta_3 + \sin^2\tfrac{1}{2}\theta_2\cos^2\tfrac{1}{2}\theta_3] + \sin^2\tfrac{1}{2}\theta_1\sin\theta_2\sin\theta_3(b\beta^* + b^*\beta)]/4|b||\beta|\,, \tag{1.32c}$$

$$(\rho_\omega)_{10} = (\rho_\omega)_{01}^* = i\sin\theta_1[ab\beta^*\sin\tfrac{1}{2}\theta_2\sin\tfrac{1}{2}\theta_3/|b||\beta| - a\cos\tfrac{1}{2}\theta_2\cos\tfrac{1}{2}\theta_3]/2|a|\,, \tag{1.32d}$$

$$(\rho_\omega)_{20} = (\rho_\omega)_{02}^* = -\frac{\sin\theta_1}{2|a|}\left[\frac{a\beta\cos\tfrac{1}{2}\theta_2\sin\tfrac{1}{2}\theta_3}{|\beta|} + \frac{ab\sin\tfrac{1}{2}\theta_2\cos\tfrac{1}{2}\theta_3}{|b|}\right], \tag{1.32e}$$

$$(\rho_\omega)_{21} = (\rho_\omega)_{12}^* = \frac{-i\beta\sin^2\tfrac{1}{2}\theta_1\cos\theta_2\sin\theta_3}{2|\beta|} - \frac{ib\sin^2\tfrac{1}{2}\theta_1\sin\theta_2\cos^2\tfrac{1}{2}\theta_3}{2|b|} + \frac{ib^*\beta^2\sin^2\tfrac{1}{2}\theta_1\sin\theta_2\sin^2\tfrac{1}{2}\theta_3}{2|b||\beta|^2}$$
$$= (T_\omega)_{21}^{(1)} + (T_\omega)_{21}^{(2)} + (T_\omega)_{21}^{(3)}\,. \tag{1.32f}$$

Here β is the equivalent of b for the third excitation pulse, i.e.,

$$\beta = -p_{21}\mathcal{E}_2'\exp(i\vec{k}_2'\cdot\vec{r}_3)\,,$$

where $\vec{r}_3$ is the atomic position at the time of the third pulse.

There are two points to discuss. First, although each off-diagonal element $(\rho_\omega)_{ij}$ has a certain overall magnitude and relative phase, it is here decomposed into a series of "memory terms" $(T_\omega)_{ij}^{(1)}, (T_\omega)_{ij}^{(2)}, \ldots$ whose relative phases are, as indicated by the phase factors, determined by the excitation fields in different ways. By way of example, this decomposition has been written out explicitly in Eq. (1.32f). This decomposition is important because, as we will see below, in a gaseous sample of atoms a necessary condition for coherent emission to occur at a particular time on the $(i$-$j)$th transition is that at least one of the memory terms $(T_\omega)_{ij}^{l}$, expressed as a function of the instantaneous position $\vec{r}(t)$, be independent or nearly independent of atomic velocity $\vec{v}$. Thus an analysis of the behavior of each individual $(T_\omega)_{ij}^{l}$ as a function of t, $\vec{r}(t)$, and $\vec{v}$ will tell us when coherent emission is *possible*. Second, the $(\rho_\omega)_{11}$ and $(\rho_\omega)_{22}$ diagonal elements contain the quantity $b\beta^* + b^*\beta$. Using the definitions of b and β, and assuming that $\vec{k}_2 \| \vec{k}_2' \| \vec{z}$, and $k_2 = k_2'$, we have

$$b\beta^* + b^*\beta \propto 2\cos[k_2(z_3 - z_2)] = 2\cos[k_2 v_z(t_3 - t_2)]\,, \tag{1.33}$$

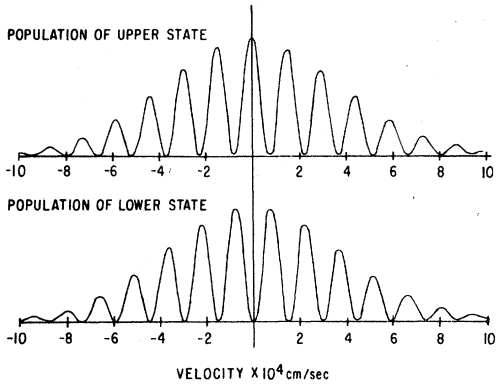

FIG. 3. Modulation of population in states $|1\rangle$ (lower) and $|2\rangle$ (upper) as a function of v_z, the z component of thermal velocity, after excitation by two pulses propagating along $\hat{z}$ resonant with the $|2\rangle - |1\rangle$ transition (see text). In generating this figure it is assumed that the temporal separation of the two excitation pulses is 4 nsec. Longer separations produce more rapid modulation of the population as a function of v_z. The envelope of the modulation represents the Doppler distribution of velocities (characteristic of Na at 400 K) which are present in $|1\rangle$ before the two $|2\rangle - |1\rangle$ excitation pulses.

where z_2 (z_3) is the position of the atom along the z axis during the second (third) pulse, which occurs at time t_2 (t_3), and v_z is the constant z component of the atom's thermal velocity. Eq. (1.33) implies that the population in both states $|1\rangle$ and $|2\rangle$ is modulated as a function of v_z. Figure 3 depicts the population in these states as a function of v_z for the case of maximum modulation ($\theta_1 = \pi$, $\theta_2 = \frac{1}{2}\pi$, and $\theta_3 = \frac{1}{2}\pi$). This modulation can be appreciated by means of a simple classical example. When a pendulum is at rest (state $|1\rangle$) all driving impulses of equal magnitude are equivalent to it. Thus the first pulse on the $|2\rangle - |1\rangle$ transition excites all the atoms equivalently. Once the pendulum is in motion, however, both the magnitude of the driving impulse and its phase relative to that of the pendulum are important. Thus the second impulse (pulse on the $|2\rangle - |1\rangle$ transition) either excites the pendulum (the atom into state $|2\rangle$) or deexcites it (into state $|1\rangle$), depending on its relative phase. In the case we consider here of an atom in a gaseous sample, the relative phase between the two impulses is determined by the distance traveled by the atom in the interval between the two pulses. Two excitation pulses in succession on a particular transition generally produce population modulation. This effect, which is responsible for the Ramsey fringe effect,[22] will be shown below to bring about a certain class of echo phenomena as well.

D. Phase matrix

Eqs. (1.19) and (1.26) provide a straightforward recipe for calculating ρ_ω; however, in cases of multiple-pulse excitation the algebraic complexity of the calculation can be burdensome. To simplify the calculation we note that, except for questions of magnitude, the phase factors appearing in ρ_ω completely determine the characteristics of a sample's coherent emission. Thus in many cases only the phase factors of ρ_ω need be calculated. This can be accomplished by setting the coefficients of the phase factors in M_R equal to unity and using the resulting matrix M_p given by

$$M_p = M_p^{-1} = \begin{pmatrix} 1 & a^* & a^*b^* \\ a & 1 & b^* \\ ab & b & 1 \end{pmatrix} \tag{1.34}$$

in Eq. 1.19. We term the modified "density matrix" ρ_p which results the *phase matrix*, since its elements are composed solely of phase factors. As an example, the phase matrix after the three excitation pulses of Fig. 2(c) is simply

$$\rho_p = \begin{pmatrix} 1 & a^* + a^*b^*\beta & a^*\beta^* + a^*b^* \\ a + ab\beta^* & 1 + (b\beta^* + b^*\beta) & b^* + \beta^* + b\beta^{*2} \\ a\beta + ab & b + \beta + b^*\beta^2 & 1 + (b\beta^* + b^*\beta) \end{pmatrix}. \tag{1.35}$$

Here a, b, and β are defined as for Eq. (1.32). In calculating Eq. (1.35), all products of a phase factor and its conjugate were set equal to unity; however, care was taken not to set such products as $b\beta^*$ equal to unity. It is seen that in the phase matrix the memory terms are simple products of phase factors; e.g., in Eq. (1.35) $T_{12}^{(1)} = b^*$, $T_{12}^{(2)} = \beta^*$, and $T_{12}^{(3)} = b(\beta^*)^2$.

Summarizing the results of Secs. IC and ID, we have applied the formalism of Secs. IA and IB to calculate the state of an atom after it is excited by several example pulse sequences. We have shown how the individual density-matrix elements of the atom should be decomposed into what we have called "memory terms," whose velocity dependence, as we will show below, determine the time at which coherent emission is possible. We have indicated that diagonal density-matrix elements may contain memory terms as well, so that the dependence of atomic population on velocity may lead to coherent emission. Finally, we have shown how the memory terms may be followed in what we have called a "phase matrix," which is a simplified density matrix in which only the phases, but not the magnitudes, of the memory terms appear.

II. COHERENT EMISSION

A. Basic requirements

In Sec. I we developed a general formalism which permits the calculation of the density matrix of a single atom after an arbitrary excitation sequence. Here, in Sec. II, we focus our attention on the nature of, and conditions governing, the coherent emission from an optically thin, Doppler-broadened sample of atoms which is large compared to the wavelength of the emitted radiation. We will see that the single-atom density matrix of Sec. I contains all the information needed to determine the characteristics of the sample's coherent emission.

In the semiclassical picture the total field emitted from a sample is simply the sum of the fields from the atoms individually. In a sample small compared to the wavelength λ of the emitted radiation, the degree to which the sample's emission is "coherent" depends on the degree to which the individual radiators (atoms) have the same phase. In a sample large compared to λ, the same basic criterion applies except that for coherent emission to occur it is also necessary that the average phase at each point varies with position in such a way that a traveling wave will remain in phase with the radiators it is passing.

To transform these qualitative remarks into quantitative results for a Doppler-broadened gaseous sample we note that the phase of the radiation emitted by each atom on the $(i\text{-}j)$th transition is determined by the phase of its dipole moment for that transition, $\mathcal{O}_{ij}$, and that we may obtain the phase of $\mathcal{O}_{ij}$ from both the ij and ji elements of each atom's laboratory-frame density matrix, using the equality $\mathcal{O}_{ij}=p_{ij}\rho_{ji}+p_{ji}\rho_{ij}$. Thus, by examining the phase information in the memory terms T^l_{ij} (T^l_{ji}) of ρ_{ij} (ρ_{ji}), we can determine the coherence properties of the sample. The analysis is facilitated by the fact that an arbitrary memory term T^l_{ij} of ρ_{ij} is proportional to an overall phase factor

$$\exp(i\varphi^l_{ij})=\exp\left[i\left(\sum_{m=1}^{n} c_m\vec{\kappa}_m\cdot\vec{r}_m-\omega_{ij}t\right)\right], \quad (2.1)$$

where the summation runs over the n phase factors associated with the T^l_{ij} memory term, $\vec{r}_m$ is the location of the atom during the mth excitation pulse at time t_m, $\vec{\kappa}_m$ is the wave vector of the mth excitation pulse, $c_m=\pm1$ or ±2, and $\omega_{ij}=\Omega_i-\Omega_j$. The constant $c_m=\pm2$ when the term contains a phase factor squared, as in Eq. (1.32f). We assume Eq. (2.1) is arranged such that $t_1<t_2<\cdots<t_n$. Consider the atoms at a particular point $\vec{r}$ in the sample at a time $t>t_n$. For each atom at $\vec{r}$ the relative phase of a memory term T^l_{ij} can be written as in Eq. (2.1). For a particular atom with constant velocity $\vec{v}$ the positions $\vec{r}_m$ can be related to $\vec{r}$ by

$$\vec{r}_m=\vec{r}-\vec{v}(t-t_m). \quad (2.2)$$

Substituting Eq. (2.2) into Eq. (2.1), we have

$$\exp(i\varphi^l_{ij})=\exp\left[i\vec{r}\cdot\left(\sum_{m=1}^{n} c_m\vec{\kappa}_m\right)-i\vec{v}\cdot\left(\sum_{m=1}^{n} c_m\vec{\kappa}_m(t-t_m)\right)-i\omega_{ij}t\right]. \quad (2.3)$$

If φ^l_{ij}, expressed in terms of $\vec{r}$ as in Eq. (2.3), is at a certain time nearly independent of $\vec{v}$, then we say the sample has *local coherence* at that time. The magnitude of the total radiating dipole moment $\mathcal{O}^l_{ij}$ at $\vec{r}$, corresponding to T^l_{ij}, is proportional to the sum of $\exp(i\varphi^l_{ij})$ over all atoms at $\vec{r}$. This sum is equivalent to the integral of Eq. (2.3) over the thermal velocity distribution $n(\vec{v})$. Explicitly,

$$\bar{\mathcal{O}}^l_{ij}\propto\exp[i(\vec{k}_p\cdot\vec{r}-\omega_{ij}t)]\int d\vec{v}\,n(\vec{v})\times\exp\left[-i\vec{v}\cdot\left(\sum_{m=1}^{n} c_m\vec{\kappa}_m(t-t_m)\right)\right], \quad (2.4)$$

where

$$\vec{k}_p\equiv\sum_{m=1}^{n} c_m\vec{\kappa}_m. \quad (2.5)$$

The integral will be small unless the coefficient of $\vec{v}$ in the exponential is nearly zero. Thus the condition for complete local coherence is that

$$|\vec{R}(t)|\equiv\left|\sum_{m=1}^{n} c_m\vec{\kappa}_m(t-t_m)\right|=0. \quad (2.6a)$$

Unless Eq. (2.6a) is nearly satisfied no coherent emission can result from the memory term T^l_{ij} under consideration. If Eq. (2.6a) is only approximately satisfied we say that the local coherence is only partial.

In Eq. (2.4) the macroscopic coherence of the sample is described by the factor $\exp[i(\vec{k}_p\cdot\vec{r}-\omega_{ij}t)]$, which describes the variation of the average phase at each point as a function of $\vec{r}$. Thus the radiation emitted by the atoms at a certain location will remain in phase with the radiators it passes if it is a traveling wave with the form $\exp[i(\vec{k}_e\cdot\vec{r}-|\omega_{ij}|t)]$, where $\vec{k}_e$ satisfies $|\vec{k}_e|=|\omega_{ij}|/c$, and

$$\vec{k}_e\cong\pm\vec{k}_p. \quad (2.6b)$$

We have assumed without loss of generality that

the refractive index of the sample is 1. The + (−) sign occurs if $\Omega_i > \Omega_j$ ($\Omega_j > \Omega_i$) and signifies that the echo propagates parallel (antiparallel) to $\vec{k}_p$. We note that the condition expressed in Eq. (2.6b) is just the phase-matching condition of nonlinear optics, albeit in a somewhat different context. The phase-matching condition ensures that the coherent radiation emitted from a large sample will be highly directional. Unless otherwise stated we assume that the excitation pulses are oriented in such a fashion that Eq. (2.6b) is satisfied.

Observing the form of $|\vec{R}|$, we see that it generally is minimum for only a certain value of t. To determine this time t_e and hence the time of potential coherent emission we first use Eq. (2.6b) to rewrite $\vec{R}$, and obtain

$$\vec{R}(t) = \vec{k}_p(t - t_1) - \sum_{m=2}^{n} c_m \vec{\kappa}_m (t_m - t_1) . \tag{2.7}$$

Then, equating $d|R(t)|^2/dt = 0$ and solving for t_e, we find

$$t_e = \vec{k}_p \cdot \vec{D}/k_p^2 , \tag{2.8}$$

where $\vec{k}_p$ is given by Eq. (2.5) and

$$\vec{D} \equiv \vec{k}_p t_1 + \sum_{m=2}^{n} c_m \vec{\kappa}_m (t_m - t_1) . \tag{2.9}$$

If the time $t_e > t_n$, where t_n is the time of the last excitation pulse, if $|\vec{R}(t_e)|$ is sufficiently small, if the relevant transition is allowed, and if Eq. (2.6b) is satisfied, an echo will be emitted in the direction $\vec{k}_p$. If $t_e < t_n$ no coherent emission is possible. However, such a situation is not without physical meaning. When $t > t_n$ the atoms at each point have the relative phases they would have had were $|\vec{R}(t)|$ minimum at the time $t_e < t_n$. This might be termed a virtual echo.[23]

For memory terms T^I_{ij} which consist of only one phase factor it is found that $t_e = t_m$, where t_m refers to the time at which the phase factor was acquired. In this case the emission from the sample represents a free decay. If a memory term T^I_{ij} from either of the elements of ρ_ω corresponding to the "forbidden" $|2\rangle$-$|0\rangle$ transition is analyzed and found to satisfy Eq. (2.6a) for some t_e, the sample can only emit direct radiation through higher multipole moments.[24] However, if the sample is "probed" by an excitation pulse at t_e which transfers the population of the $|2\rangle$ ($|0\rangle$) state to the $|1\rangle$ state, the sample has immediate local coherence on the allowed $|1\rangle$-$|0\rangle$ ($|2\rangle$-$|1\rangle$) transition and may radiate coherently if Eq. (2.6b) is satisfied.

We now turn our attention to determining the magnitude of $|\vec{R}|$ at t_e. Inserting Eq. (2.8) into Eq. (2.7) it is found that

$$\vec{R}(t_e) = -\vec{D}_\perp = -[\vec{D} - \vec{k}_p(\vec{k}_p \cdot \vec{D})/k_p^2] , \tag{2.10}$$

where $\vec{D}_\perp$ represents the component of $\vec{D}$ perpendicular to $\vec{k}_p$. In the case when all the excitation pulses travel collinearly it is clear from Eqs. (2.6b) and (2.9) that $\vec{D} \,|\, \vec{k}_p$ and $\vec{D}_\perp \equiv 0$. Thus the sample rephases completely to produce maximum local coherences and hence maximum echo size. With noncollinear excitation pulses $\vec{D}_\perp$ is generally nonzero, leading to reduced local coherence. Since it is easier to detect an echo when it is not traveling collinearly with an excitation pulse, it is useful to determine whether $|\vec{D}_\perp|$ remains sufficiently small in the noncollinear case to produce an echo of reasonable size.

The decrease in echo intensity which results from a given nonzero $|\vec{D}_\perp|$ relative to the case when $|\vec{D}_\perp| = 0$ can be determined by performing the integration of Eq. (2.4). Substituting

$$n(\vec{v}) \propto \exp(-mv^2/2k_bT) , \tag{2.11}$$

where m is the mass of an atom, k_b is Boltzmann's constant, and T is the absolute temperature, into Eq. (2.4), we have

$$\bar{\mathcal{O}}^I_{ij}(|\vec{D}_\perp|)/\bar{\mathcal{O}}^I_{ij}(0) = \int_{-\infty}^{\infty} dv_x\, dv_y\, dv_z \exp[-(mv^2/2k_bT + i\vec{v}\cdot\vec{D}_\perp)] . \tag{2.12}$$

Upon evaluation of the integral this becomes

$$\bar{\mathcal{O}}^I_{ij}(|\vec{D}_\perp|)/\bar{\mathcal{O}}^I_{ij}(0) = \exp(\tfrac{1}{4}V_0^2|\vec{D}_\perp|^2) , \tag{2.13}$$

where

$$V_0 = (2k_bT/m)^{1/2} . \tag{2.14}$$

With all other factors (such as overlap volume of the excitation pulses) held constant, the intensity of the emitted radiation corresponding to the memory term T^I_{ij} vaires as $(\bar{\mathcal{O}}^I_{ij})^2$. Thus we have

$$I(|\vec{D}_\perp|)/I(0) = \exp(-\tfrac{1}{2}V_0^2|\vec{D}_\perp|^2) . \tag{2.15}$$

From Eq. (2.15) it is evident that the intensity of the emitted radiation falls off rapidly as $|\vec{D}_\perp|$ increases beyond $1/v_0$.

B. Excitation pulse requirements and absolute echo size

It is found that with all other factors (sample geometry, $\vec{D}_\perp$, etc.) held constant the echo intensity is optimized when the magnitude of the memory term T^I_{ij} responsible for the echo in maximized. Examining, for example, the density matrix represented in Eq. (1.32), we see that the memory terms are maximized when the excitation pulse areas are of order $\frac{1}{2}\pi$. Thus to determine the approximate intensity required of a Fourier-transform-limited square pulse resonant with the

$(i\text{-}j)$th transition it is only necessary to calculate the intensity $I^{ij}_{(\pi/2)}$ of a $\frac{1}{2}\pi$ pulse on the $|i\rangle$-$|j\rangle$ transition. Since the expressions have been evaluated elsewhere,[4,25] we quote the result

$$I^{ij}_{(\pi/2)} = \pi^4\hbar c/3\lambda^3_{ij}\tau^2 A_{ij}, \tag{2.16a}$$

where λ_{ij} is the wavelength of the particular transition, τ is the temporal width of the pulse, and A_{ij} is the Einstein A coefficient for the transition. Alternatively, using the oscillator strength f_{ij} of the transition, we find that $I^{ij}_{(\pi/2)}$ is given by

$$I^{ij}_{(\pi/2)} = \pi^2\hbar/24\tau^2 r_e \lambda_{ij} f_{ij}, \tag{2.16b}$$

where $r_e \equiv e^2/mc^2$ is the classical electron radius, and, ignoring the possible degeneracy of states i and j, f is related to A by $f = A\lambda^2/8\pi^2 r_e c$. For the resonance lines of the alkali metals the order of magnitude of $I_{(\pi/2)}$ is 1 W/cm^2 for a 7-nsec pulse. These power levels are clearly obtainable with available tunable dye lasers.

The intensity of the echo can be calculated by solving the classical problem of the intensity emitted by a phased array of oscillating dipoles. The amplitude and spatial arrangement of the oscillating dipoles are determined by the magnitude of the memory term of ρ responsible for the echo and the directions of the excitation pulses, respectively. Fortunately, this problem has been analyzed in detail for the case of the photon echo[4,25] and those results properly interpreted can also be applied to other types of echoes.

Let the echo be generated on the $(i\text{-}j)$th transition by atoms in a pencil-shaped sample whose cross section area s and length l satisfy the condition that the Fresnel number $(s/\lambda_{ij}l) \gg 1$. Then it is found that the number η of photons emitted in an echo is

$$\eta = \frac{3}{32\pi}(2p_0)^2 n l^2 s \lambda^2_{ij} A_{ij}\tau, \tag{2.17}$$

where n is the number density of atoms excited and p_0 is the magnitude of the memory term of ρ_ω responsible for the echo.

In deriving the expression for η it is assumed that Eq. (2.6b) is satisfied exactly, optimum excitation pulses are used throughout, and all relaxation effects are neglected. Furthermore, Eq. (2.17) becomes invalid if n is not uniform throughout the sample or a significant fraction of the stored energy is emitted. For n to be constant throughout the sample it is necessary that the sample be optically thin on all the pump transitions. Explicitly, $\alpha^{ij}_a l \ll 1$, where α^{ij}_a, the classical absorption coefficient for the $(i\text{-}j)$th transition, is given by $\alpha^{ij}_a = (3\pi/4)n\lambda^2_{ij}A_{ij}T^{*ij}_2$, with T^{*ij}_2 representing the inhomogeneous dephasing time of the $(i\text{-}j)$th transition. In the case of the photon echo for which only one transition is involved, Eq. (2.17) can be rewritten simply in terms of the $\alpha_a l$ and η_{ex}, the number of resonant photons in a $\frac{1}{2}\pi$ excitation pulse, as

$$\eta_{PE} = (\alpha_a l/\pi)^2 \eta_{ex}. \tag{2.18}$$

Although Eq. (2.18) is only valid for $\alpha_a l \ll 1$ the case of larger $\alpha_a l$ has been studied.[26] It is found that the echo peaks at $\alpha_a l \cong 1$ and at the point is somewhat smaller than the value predicted by Eq. (2.18). Thus the magnitude of a photon echo can be within approximately two orders of magnitude of a $\frac{1}{2}\pi$ pulse on the emitting transition. Eq. (2.18) fails for $\alpha_a l \gtrsim 1$ because the pump pulses are absorbed before passing through the sample.

It is not possible to give a comprehensive statement regarding the maximum size of an arbitrary trilevel echo. It is necessary to examine the conditions of validity of Eq. (2.17) with respect to n for each echo type. The maximum obtainable echo can then be estimated by calculating η for the number density at which Eq. (2.17) begins to become invalid.

The quantities appearing in Eqs. (2.16) and (2.18) must be reinterpreted in the case of non-Fourier-transform-limited pulses. It is found that the necessary non-transform-limited pulse intensity is given by $(I^{NTL}_{(\pi/2)})^{ij} \cong (\tau/\tau_L) I^{ij}_{(\pi/2)}$, where $2\pi\tau_L$ is the inverse of the spectral width of the excitation pulse and η_{ex} is given by the number of resonant photons in the non-transform-limited $\frac{1}{2}\pi$ pulse.

C. Summary

In summary, we have considered in Sec. II a model medium, consisting of a dilute sample of atoms of the type discussed in Sec. I, which is optically thin but which has a spatial extent much larger than a wavelength. We have shown that in order for coherent radiation to be emitted by this sample, two basic requirements must be fulfilled, one implying "local" coherence and the other macroscopic coherence. The second requirement is equivalent to phase matching in nonlinear optics. Free decay and echoes have been shown to be possible examples of the coherent emission. Finally, we have discussed the excitation pulse intensity requirements and the absolute size of the echo.

III. ATOMIC RELAXATION AND ECHO DECAY

Although the results presented above afford a description of the basic properties of echo effects, no account has been given of the important influence of atomic relaxation processes on echo behavior. It is found that such basic properties of echoes as the time of occurrence are not significantly affected by relaxation processes; however,

the echo intensity is reduced. This degradation of echo intensity can be utilized to obtain significant information concerning the relaxation processes responsible for it. We restrict ourselves here to a qualitative discussion of the effects of relaxation processes which occur in a gaseous medium. More detailed treatments of various aspects of echo decay in gases can be found elsewhere.[27]

As a preliminary, we discuss the means by which the sample stores the information necessary to produce an echo (echo information). We divide the interval t_{e1} between the first excitation pulse and the echo into subintervals t_{ij}, which are bounded by the times t_i of the excitation pulses. It is found that during any subinterval except t_{21} and t_{en}, where t_n is the time of the last excitation pulse, the echo information can be stored in one of two ways: (i) an ordering (with respect to a particular component of the thermal velocity and the position at time t_1 of each atom) of the phase associated with a certain two-level superposition state of the atom, or (ii) a modulation of the population in *one particular state* as a function of a given component of the thermal velocity. We term the former mode of storage "phase mediated," while we term the latter "population mediated." Population-mediated storage of echo information was discussed in Sec. IC. During the intervals t_{21} and t_{en} only phase-mediated storage is possible. Phase-mediated echo information can be converted (by an excitation pulse) to population-mediated echo information and vice versa. The final echo intensity depends on the maintainance of the echo information throughout t_{e1}. Thus any decrease in echo intensity can be written as a product of factors each of which represents the loss of echo information during a particular t_{ij}. In a gaseous sample relaxation occurs, principally due to spontaneous emission and collisions. We concentrate on collisional relaxation.

During an interval t_{ik} of population-mediated storage of echo information collisions can destroy the echo information in two ways. First, state-changing collisions can remove atoms from the information-containing energy state, and second, the modulated atomic velocity distribution can be altered by velocity-changing collisions (VCC). In the latter case the effectiveness of velocity changes of a given magnitude toward randomizing the velocity distribution depends on the temporal length of one of the preceding intervals t_{ij} (see Sec. IC). Thus given a fixed probability distribution of velocity changes occurring in the collisions, the rate at which the echo information is destroyed during t_{ik} can be dependent on t_{ij}. In fact it has been shown[16] that, by studying the t_{ij} dependence of the rate of echo information loss during t_{ik}, it is possible to infer the distribution of velocity changes occurring in the collisions, as well as to unambiguously determine the total VCC cross section (see Sec. IV B).

During intervals of phase-mediated storage of echo information the situation is more complicated. In addition to state-changing collisions and VCC we must consider the effect of phase-changing collisions (PCC), i.e., those collisions which change the phase of the relevant two-level superposition state. Considerable effort has gone into understanding the meaning of VCC and PCC and their interrelationship when experienced by an atom in a superposition state.[28] However, there is experimental evidence[1,25] which implies that the echo decay resulting from collisions occurring during an interval of phase-mediated echo information storage can be related to the widths of collisionally broadened absorption lines which are observed in traditional absorption linewidth measurements.

IV. DESCRIPTION OF SOME PARTICULARLY INTERESTING ECHO EFFECTS

A. Photon echoes

The two-pulse photon echo[4] has been dealt with extensively both experimentally[17,25,29] and theoretically[30] by others and thus provides a natural first application of the present formalism. We first obtain the density matrix (or phase matrix) for a two-level atom after two excitation pulses. The two levels can be considered to be the levels $|0\rangle$ and $|1\rangle$ of the three-level atom of Fig. 1(a). Figure 4 shows the excitation scheme and angular

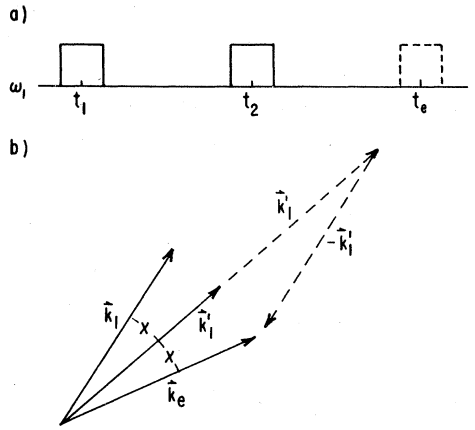

FIG. 4. (a) The two excitation pulses (solid lines) and the echo involved in a two-pulse two-level (photon) echo. (b) The angular configuration of the first ($\vec{k}_1$) and second ($\vec{k}_1'$) excitation pulses and the echo ($\vec{k}_e$). The two excitation pulses are at an angle χ with respect to each other. It is apparent that for $\chi > 0$, $2\vec{k}_1' - \vec{k}_1 \neq \vec{k}_e$ and the echo is not phase matched. For small χ the phase mismatch is minimum when the echo is at an angle of 2χ with respect to $\vec{k}_1$.

orientation of the excitation pulses. Pulse 1 (2) with wave vector $\vec{k}_1$ ($\vec{k}_1'$) and phase factor $a = -p_{10}\mathcal{E}_1 \exp(i\vec{k}_1\cdot\vec{r}_1)$ [$\alpha = -p_{10}\mathcal{E}_1' \exp(i\vec{k}_1'\cdot\vec{r}_2)$] occurs at time t_1 (t_2). The wave vectors $\vec{k}_1$ and $\vec{k}_1'$ make an angle χ with respect to each other. Using the 2×2 upper left-hand corner of Eq. (1.28) as the initial density matrix along with Eq. (1.18), we find that after the second pulse

$$(\rho_\omega)_{00} = \cos^2\tfrac{1}{2}\theta_1 \cos^2\tfrac{1}{2}\theta_2 + \sin^2\tfrac{1}{2}\theta_1 \sin^2\tfrac{1}{2}\theta_2 - \frac{\sin\theta_1 \sin\theta_2}{4|a||\alpha|}(\alpha^* a + \alpha a^*), \tag{4.1a}$$

$$(\rho_\omega)_{10} = (\rho_\omega)_{01}^* = \frac{-ia\sin\theta_1 \cos^2\tfrac{1}{2}\theta_2}{2|a|} - \frac{i\alpha\cos\theta_1 \sin\theta_2}{2|\alpha|} + \frac{i\alpha^2 a^* \sin\theta_1 \sin^2\tfrac{1}{2}\theta_2}{2|a||\alpha|^2}, \tag{4.1b}$$

$$(\rho_\omega)_{11} = \cos^2\tfrac{1}{2}\theta_1 \sin^2\tfrac{1}{2}\theta_2 + \sin^2\tfrac{1}{2}\theta_1 \cos^2\tfrac{1}{2}\theta_2 + \frac{\sin\theta_1 \sin\theta_2}{4|a||\alpha|}(\alpha^* a + \alpha a^*). \tag{4.1c}$$

The memory term which produces the echo is

$$(T_\omega)_{10}^{\mathrm{PE}} = ia^*\alpha^2 \sin\theta_1 \sin^2\tfrac{1}{2}\theta_2 / 2|a||\alpha|^2. \tag{4.2}$$

The other two memory terms of $(\rho_\omega)_{10}$ correspond to free decay after the first and second pulses, respectively. From the expression for $(T_\omega)_{10}^{\mathrm{PE}}$ and Eq. (2.1) we see that

$$c_1\vec{\kappa}_1 = -\vec{k}_1, \tag{4.3a}$$

$$c_2\vec{\kappa}_2 = 2\vec{k}_1'. \tag{4.3b}$$

Since $k_1 = k_1' = k_e = \omega_1/c$, it is impossible to satisfy the phase-matching condition Eq. (2.6b) which requires that $2\vec{k}_1 - \vec{k}_1 = \vec{k}_e$ if $\chi > 0$. Thus for $\chi \neq 0$ the echo will suffer some degradation due to the fact that the emitted echo signal will not remain in phase with the atoms it passes throughout the sample length. For small χ this degradation is at a minimum along the direction $\vec{k}_e$ which minimizes $|\vec{k}_e - 2\vec{k}_1' + \vec{k}_1|$. Since Eq. (2.6b) is not satisfied, the expression for the echo time Eq. (2.8) is only approximately correct. However, for small χ the error is negligible. Using Eqs. (2.8) and (4.3), we find

$$t_e \cong t_1 + 2(t_2 - t_1)\cos\chi \tag{4.4}$$

to be the time of maximum rephasing. The degree of rephasing is found by using Eqs. (2.10) and (2.15). For small χ

$$|\vec{D}_\perp|^2 = 2(t_2 - t_1)^2 k_e^2 \chi^2, \tag{4.5}$$

and the echo intensity is reduced owing to incomplete rephasing according to

$$I_e(\chi)/I_e(\chi = 0) = \exp(-v_0^2(t_2 - t_1)^2 k_e^2 \chi^2). \tag{4.6}$$

Note that the decrease in echo size due to imperfect phase-matching is not accounted for here. As an example of the effect of Eq. (4.6) consider the case of photon echoes on the $3S$-$3P$ transition in sodium vapor, where $k_e = 2\pi/(5.89\times 10^{-5}$ cm), $v_0 = 5.4\times 10^4$ cm/sec for a temperature of 400 °K, $(t_2 - t_1) = 50$ nsec, and $\chi = 0.02$ rad ($\cong 1°$). It is found that $I_e(0.02)/I_e(0) = e^{-33}$. Thus the echo is rapidly destroyed as χ is increased from zero. Note, however, that if $t_2 - t_1$ is shortened, a considerably smaller decrease takes place for a given χ. This fact has recently been utilized by Hu and Gibbs[31] to detect picosecond photon echoes [32] on the sodium transition discussed above. When $\chi = 0$ both the rephasing and phase-matching conditions are satisfied exactly. The results obtained here concerning the photon echo agree with those obtained in the previous treatments mentioned above.

B. Stimulated photon echoes

As in the case of the photon echo, the three-pulse stimulated photon (SP) echo is a well-known phenomenon.[3,5] We find,[16] however, that the SP echo has a number of interesting and useful features which have previously gone unnoticed.

1. Simple picture

In its simplest form the SP echo is produced by three excitation pulses resonant with a single transition [see Fig. 5(a) for nomenclature]. However, we find that [as shown in Fig. 5(b)] the third pulse may also be resonant with a different transition. A simple picture can be used to understand the formation and principal features of the SP echo. Consider the action of the first two pulses (for this discussion $\vec{k}_1 = \vec{k}_1' \,||\, \hat{z}$). The two-level density matrix after the first two pulses is given by Eq. (4.1). The appearance of the $\alpha^* a + \alpha a^*$ factor in Eqs. (4.1a) and (4.1c) indicates [see Eq. (1.33) and accompanying discussion] that the population in both the upper, $|1\rangle$, and lower $|0\rangle$, state is modulated as a function of the $\hat{z}$ component of velocity (z velocity). If we assume [in Eq. (4.1)] that $\theta_1 = \theta_2 = \frac{1}{2}\pi$, the z velocity distribution of atoms in either state can be written as

$$n'(v_z) = c_0 \exp(-mv_z^2/2k_bT) f(\tfrac{1}{2}k_1 v_z t_{21}), \tag{4.7}$$

where c_0 is a constant, $t_{ij} = t_i - t_j$, $f \equiv \sin^2$ for state $|0\rangle$, and $f \equiv \cos^2$ for state $|1\rangle$. The exponential envelope represents the normal thermal distribution of v_z. It is the modulated z velocity distribution in *either* state $|0\rangle$ *or* $|1\rangle$ *separately* which contains the information necessary to produce the SP echo.

To see how the third excitation pulse acts to create an echo, we imagine that we are somehow

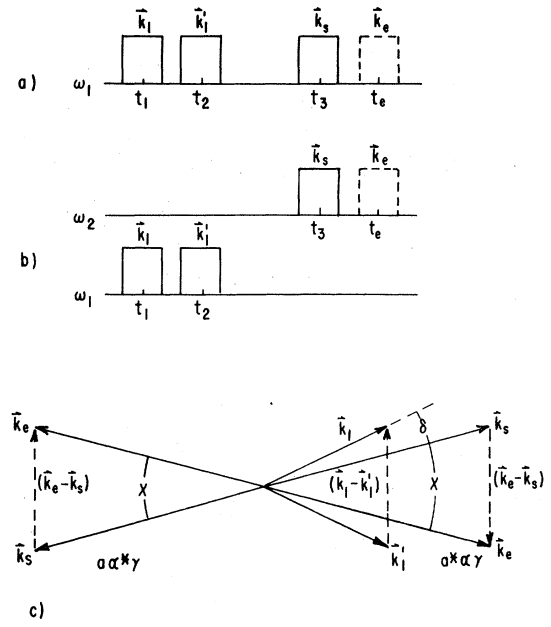

FIG. 5. (a) Excitation pulses (solid lines) and echo involved in the usual two-level stimulated photon echo. (b) The excitation pulses and echo which result when the third excitation pulse is resonant with a different transition involving only one of the initial two levels. In this case the "information" responsible for the echo is stored in only one atomic state between t_2 and t_3. (c) The phase-matched spatial orientation of the excitation pulses and the echo. Note that the third pulse ($\vec{k}_s$) and echo ($\vec{k}_e$) can propagate in the same or opposite direction as the first two excitation pulses ($\vec{k}_1$ and $\vec{k}_1'$).

able to obtain a sample of atoms all of which are in state $|0\rangle$ but whose z velocity distribution is modulated as shown in Eq. (4.7) and Fig. 3. The third pulse excites the atoms in $|0\rangle$ into a superposition between the $|0\rangle$ and $|1\rangle$ states. Since the pulse excites the atoms coherently, the atoms at each point initially radiate in phase. This results in a free decay signal. Being Doppler shifted from each other in frequency, the atoms dephase and the free decay terminates. However, because of the modulation of the z velocity distribution (and hence the frequency distribution), it is found that the atoms are again partially in phase at a later time and emit the SP "echo". More quantitatively, the time evolution of the field emitted from the atoms at one representative point in the sample is obtained from the Fourier transform of the z velocity (frequency) distribution.

$$E_{\rm tot}(t)=\int_{-\infty}^{\infty} n'(v_z)E(v_z,t)dv_z$$

$$=c_0'\int_{-\infty}^{\infty}\exp(-mv_z^2/2k_bT)\sin^2(\tfrac{1}{2}k_1v_zt_{21})\times\exp[-i(\omega_1+\kappa v_z)t]dv_z, \qquad (4.8)$$

where $E(v_z,t)$ is the field emitted by a single atom, $t=0$ at the time of the third pulse, c_0' is a constant, and $\kappa\equiv\vec{k}_s\cdot\hat{z}$. We find

$$E_{\rm tot}(t)=c_0''\exp(-i\omega_1 t)\{\exp(-\tfrac{1}{4}\kappa^2t^2v_0^2)+\tfrac{1}{2}\exp[-\tfrac{1}{4}(\kappa t-k_1t_{21})^2v_0^2]+\tfrac{1}{2}\exp[-\tfrac{1}{4}(\kappa t+k_1t_{21})^2v_0^2]\}, \qquad (4.9)$$

where $v_0\equiv(2k_bT/m)^{1/2}$ and c_0'' is a constant. The first term of Eq. (4.9) corresponds to the usual free decay from a thermal (Gaussian) distribution of z velocities. The second (third) term, which peaks at $t=k_1t_{21}/\kappa$ ($t=-k_1t_{21}/\kappa$) represents the SP echo when $\vec{k}_s\|\hat{z}$ ($\vec{k}_s\|-\hat{z}$). The description of the SP echo as free decay shows clearly how modulation of the z velocity distribution [Eq. (4.7)] in a single state can lead to an echo.

We can immediately appreciate some interesting aspects of the stimulated echo. (i) An echo will occur if the third pulse excites a transition which has *either* level $|0\rangle$ *or* level $|1\rangle$ as a terminal level.[33] From the expression for the echo time above we see that it will vary with the ratio k_1/k_s. (ii) If pulse 3 excites the $|0\rangle$-$|1\rangle$ transition and both levels are equally populated, the free decay at $t=0$ vanishes, but the intensity of the SP echo is four times as large as it would be if one of the levels was empty. (iii) The third excitation pulse can propagate parallel or antiparallel to the first two pulses. (iv) As long as z velocity modulation exists an SP echo can be produced. The electric field of an SP echo created by using only the z-velocity modulation in level $|1\rangle$ (assumed to be an excited state) will decay as a function of t_{32} at the same rate as the population in $|1\rangle$. In contrast, an SP echo generated from z velocity modulation in $|0\rangle$ (assumed to be a ground state) can last indefinitely. As long as all the population in $|1\rangle$ does not recombine with the population in $|0\rangle$ [thus destroying the z velocity modulation; see Eq. (4.7)], an SP echo can be created. The appearance of hyperfine structure or magnetic degeneracy in $|0\rangle$ can result in SP echoes which are independent of t_{32} for as long as the atoms do not diffuse out of the excitation region. (v) If the population in $|1\rangle$ decays to state $|x\rangle$, the z velocity distribution in $|x\rangle$ is modulated (neglecting radiation reaction). Thus if the third excitation pulse excites a transition with $|x\rangle$ as a terminal level an SP echo can occur.

2. *Detailed analysis*

We now apply the methods of Secs. I and II to analyze the SP echo. We assume that pulse 3 is resonant with the $|i\rangle$-$|j\rangle$ transition, where it is understood that at least one of the terminal levels

is $|0\rangle$ or $|1\rangle$. We need to obtain the $(\rho_\omega)_{ij}$ element of the density matrix after pulse 3. This is made easy by the fact (shown by the free-decay model) that after pulse 2 the SP "echo information" resides solely in the population of the $|0\rangle$ or $|1\rangle$ level—not in their superposition. Thus the action of pulse 3 can be calculated by using a simple two-level density matrix describing the $|i\rangle$ and $|j\rangle$ levels. The off-diagonal elements of this two-level ρ_ω before pulse 3 are zero, while the diagonal ones simply represent the population in the levels $|i\rangle$ and $|j\rangle$ after pulse 2. For example, if $|i\rangle = |0\rangle$ and $|j\rangle = |1\rangle$ [Fig. 5(a)] the diagonal elements of the two-level ρ_ω are given by Eqs. (4.1a) and (4.1c). If $|i\rangle = |1\rangle$ and $|j\rangle$ is a higher energy state, initially unpopulated, then $(\rho_\omega)_{00}$ is given by Eq. (4.1c) and $(\rho_\omega)_{11} = 0$. We assume that the rows and columns of the two-level ρ_ω are arranged so that the population in the state of lower energy appears in the $(\rho_\omega)_{00}$ position. In this case the phase factor of pulse 3 has the form $\gamma \propto \exp(i\vec{k}_s \cdot \vec{r})$.

After applying the M_R matrix for pulse 3 [Eqs. (1.18) and (1.26)], we find that $(\rho_\omega)_{ij}$ contains the two memory terms

$$(T_\omega)_{ij} \propto \frac{ia\alpha^*\gamma \sin\theta_1 \sin\theta_2 \sin\theta_3}{8|a||\alpha||\gamma|}, \tag{4.10a}$$

$$(T_\omega)'_{ij} \propto \frac{ia^*\alpha\gamma \sin\theta_1 \sin\theta_2 \sin\theta_3}{8|a||\alpha||\gamma|}, \tag{4.10b}$$

where γ and θ_3 are respectively the phase factor and area of pulse 3; the other quantities are defined in Eq. (4.1).

Using the expressions for the phase factors a and α given preceding Eq. (4.1) and the expression for γ above, we find that the $c_i\vec{\kappa}_i$ coefficients of Eq. (2.1) are given by

$$c_1\vec{\kappa}_1 = \pm\vec{k}_1, \tag{4.11a}$$

$$c_2\vec{\kappa}_2 = \mp\vec{k}'_1, \tag{4.11b}$$

$$c_3\vec{\kappa}_3 = \vec{k}_s, \tag{4.11c}$$

where here and in the following equations the upper (lower) signs correspond to the $a\alpha^*\gamma$ ($a^*\alpha\gamma$) term in Eq. (4.10). The SP-echo phase-matching conditions [Eq. (2.6b)] derived from the two memory terms of Eq. (4.10) can be written as

$$\vec{k}_e - \vec{k}_s = \vec{k}_1 - \vec{k}'_1 \quad (a\alpha^*\gamma), \tag{4.12a}$$

$$\vec{k}_e - \vec{k}_s = -(\vec{k}_1 - \vec{k}'_1) \quad (a^*\alpha\gamma). \tag{4.12b}$$

We discuss here only the two spatial orientations of the excitation pulses shown in Fig. 5(c). It can be seen that, unlike the photon echo, the SP echo can be phase-matched with noncollinear excitation pulses. The effect of excitation-pulse noncollinearity on rephasing will be considered below.

Using Eqs. (2.9) and (4.11), we find

$$\vec{D} = \vec{k}_e t_1 \mp \vec{k}'_1(t_2 - t_1) + \vec{k}_s(t_3 - t_1), \tag{4.13}$$

and the time of the echo is found to be

$$t_e = t_1 \mp (\vec{k}_e \cdot \vec{k}_1/k_e^2)(t_2 - t_1) + (\vec{k}_e \cdot \vec{k}_s/k_e^2)(t_3 - t_1). \tag{4.14}$$

Since it is necessary to have $t_e > t_3$ for an echo to be emitted, we see that the $a\alpha^*\gamma$ ($a^*\alpha\gamma$) memory term produces an echo only when the third pulse counterpropagates (copropagates) with the first two excitation pulses. The spatial orientations of the excitation pulses and echo shown in Fig. 5(c) provide for $t_e > t_3$ as well as satisfying the phase-matching condition Eq. (4.12). If χ and $\delta \ll 1$ we have

$$t_e = t_1 + (k'_1/k_e)(t_2 - t_1)\cos(\chi + \delta) + (t_3 - t_1)\cos\chi. \tag{4.15}$$

When $\chi = \delta = 0$ and $t_1 = 0$, we have $t_e = (k'_1 t_2/k_e) + t_3$, which agrees with the result obtained from the free-decay model.

We use Eq. (2.10) with $t_1 = 0$ to determine the effect of excitation-pulse noncollinearity on the rephasing of the SP echo. We have (where "ctp" and "cp" denote counter- and copropagation, respectively)

$$\vec{D}_\perp^{\,\mathrm{ctp}}(a\alpha^*\gamma) = -[\vec{k}'_1 + \vec{k}_e(k'_1/k_e)\cos\delta]t_2 + (\vec{k}_s - \vec{k}_e\cos\chi)t_3, \tag{4.16a}$$

$$\vec{D}_\perp^{\,\mathrm{cp}}(a^*\alpha\gamma) = [\vec{k}'_1 - \vec{k}_e(k'_1/k_e)\cos\delta]t_2 + (\vec{k}_s - \vec{k}_e\cos\chi)t_3. \tag{4.16b}$$

If χ and $\delta \ll 1$, both expressions give

$$|\vec{D}_\perp|^2 = (k_s t_3 \chi - k'_1 t_2 \delta)^2. \tag{4.17}$$

3. *Decay of the* SP *echo due to velocity-changing collisions*

The action of "echo-atom"–foreign-gas-atom collisions during t_{32} on the population-mediated SP echo information leads to foreign-gas-induced decay of the SP echo which has interesting and useful aspects.[34] While a sophisticated analysis of this relaxation problem might follow along the lines of the works in Ref. 35, our method is similar to those described in the review article by Breene.[36]

We analyze the foreign-gas-induced decay of the SP echo while assuming the following: (i) The third excitation pulse excites only one of the two levels coupled by the first two excitation pulses. This implies that during t_{32} the effect of collisions on atoms in only one state, which for convenience we designate $|e\rangle$, contributes to SP echo decay; (ii) State-changing collisions do not significantly affect the population in state $|e\rangle$ during t_{32}; (iii) All atoms which experience a collision during the phase-mediated (see Sec. III) intervals t_{21} and t_{e3} do not participate in the echo. The resulting sim-

ple exponential decay of the SP echo intensity with foreign-gas pressure P can be measured independently by means of photon echoes and removed from the overall SP echo decay rate to determine the decay due to collisions in the interval t_{32} alone; (iv) All excitation pulses and the resulting SP echo are collinear ($\vec{k}_i \| \pm\hat{z}$, $i=1,2,s,e$). Because of assumption (ii) collisions during t_{32} can only disturb the SP echo information by causing a thermalization of the periodically modulated distribution of z velocities of the atoms in state $|e\rangle$.

The third excitation pulse places atoms which were in state $|e\rangle$ during t_{32} into a superposition state, the phase of which is determined by the phase of the electric field of the third excitation pulse at the location of interaction. Because of atomic motion, most of the atoms at an arbitrary location z_0 at a time $t>t_3$ were excited elsewhere and will generally have phases different from one another. We note that

$$\bar{\mathcal{P}} \propto \langle \exp(i\varphi_j) \rangle , \tag{4.18}$$

where $\bar{\mathcal{P}}$ denotes the macroscopic dipole moment at time t, the brackets represent an average over all atoms at z_0, and φ_j is the phase of an arbitrary atom at z_0 at time t relative to an atom which was excited at z_0. Since a given atom at z_0 at time t, which has a velocity v_z^j, was excited at $z'=z_0 - v_z^j(t-t_3)$, and since the phase of the electric field of the third pulse varies as $\exp(ik_e z)$, we find (using $k_s=k_e$) that $\varphi_j=-k_e v_z^j(t-t_3)$. The analysis of the SP echo above indicates that in the absence of VCC $\bar{\mathcal{P}}$ will be large at a later time t_e. We term the atoms at z_0 at time t_e in the absence of VCC as the "original" group.

In the presence of VCC the jth atom acquires a total z velocity change during t_{32} given by

$$\Delta v_T^j = \sum \Delta v_i^j , \tag{4.19}$$

where the sum is over the z velocity changes experienced in individual collisions. The velocity changes result in the presence of a "new" group of atoms at z_0 at the time t_e. The z velocity of the jth atom of the new group of atoms at z_0 at time t_e can be written as $v_z^{j\prime}+\Delta v_T^j$, where $v_z^{j\prime}$ is the original unperturbed z-velocity of the atom. The phase of atom j with respect to an atom excited at z_0 is $\varphi_j'+\Delta\varphi_j=-k_e(v_z^{j\prime}+\Delta v_T^j)t_{e3}$. Accordingly, the macroscopic dipole moment $\bar{\mathcal{P}}'$ of the new group of atoms at z_0 at time t_e is proportional to $\langle \exp[i(\varphi_j'+\Delta\varphi_j)] \rangle$. Assuming that $v_z^{j\prime}$ and Δv_T^j are uncorrelated, we have

$$\langle \exp[i(\varphi_j'+\Delta\varphi_j)] \rangle = \langle \exp(i\varphi_j') \rangle \langle \exp(i\Delta\varphi_j) \rangle . \tag{4.20}$$

Since the distribution of $v_z^{j\prime}$ among the new group of atoms is necessarily identical to the distribution of v_z^j among the original atoms, we have $\langle \exp(i\varphi_j') \rangle = \langle \exp(i\varphi_j) \rangle$. Furthermore, since the SP echo intensity $I_e \propto (\bar{\mathcal{P}}')^2$, we see immediately that

$$I_e \propto \langle \exp(i\Delta\varphi_j) \rangle^2 = \langle \exp(-ik_e \Delta v_T^j t_{e3}) \rangle^2 . \tag{4.21}$$

In accordance with the assumed random nature of the collisions, the probability $W(N)$ that a given atom will experience N collisions is given by a Poisson distribution

$$W(N) = (n v_r \sigma t_{32})^N \exp(-n v_r \sigma t_{32})/N! , \tag{4.22}$$

where n is the foreign-gas density, $v_r = (8k_bT/\pi\mu)^{1/2}$ is the echo-atom–foreign-gas-atom relative velocity, μ is the echo-atom–foreign-gas-atom reduced mass, σ is the total VCC cross section, and $nv_r\sigma t_{32}$ is the average number of collisions during t_{32}. We assume the existence of a scattering kernel $f(\Delta v_i)$, symmetric about $\Delta v_i=0$, which gives the probability that a single collision will introduce a z velocity change Δv_i. Then, expressing the average of $\langle \exp(i\Delta\varphi_j) \rangle^2$ over all atoms at z_0 as an equivalent average over all possible $\Delta\varphi_j$ of a single atom, we have

$$\begin{aligned} &\langle \exp(-ik_e \Delta v_T t_{e3}) \rangle \\ &\quad = W(0) + \sum_{N=1}^{\infty} W(N) \\ &\qquad \times \int_{-\infty}^{\infty} \prod_{i=1}^{N} \exp(-ik_e \Delta v_i t_{e3}) f(\Delta v_i) d(\Delta v_i) . \end{aligned} \tag{4.23}$$

Since the Δv_i are considered independent

$$\begin{aligned} &\langle \exp(-ik_e \Delta v_T t_{e3}) \rangle \\ &\quad = W(0) + \sum_{N=1}^{\infty} W(N) \\ &\qquad \times \left(\int_{-\infty}^{\infty} \exp(-ik_e \Delta v_i t_{e3}) f(\Delta v_i) d(\Delta v_i) \right)^N . \end{aligned} \tag{4.24}$$

Performing the summation indicated and using Eq. (4.22), we find that the SP echo intensity decays with foreign-gas density as

$$\begin{aligned} &I_e(n) \\ &\quad = I_0 \exp\left[-2nv_r\sigma t_{32} \right. \\ &\qquad \left. \times \left(1 - \int_{-\infty}^{\infty} \exp(-ik_e \Delta v_i t_{e3}) f(\Delta v_i) d(\Delta v_i) \right) \right] . \end{aligned} \tag{4.25}$$

As a function of foreign-gas pressure, which is the more directly observable quantity, we find

$$I_e(P) = I_0 \exp(-\beta' P) , \tag{4.26}$$

where

$$\begin{aligned} \beta' = 2\frac{n_0}{P_0} v_r \sigma t_{32} \\ \times \left(1 - \int_{-\infty}^{\infty} \exp(-ik_e \Delta v_i t_{e3}) f(\Delta v_i) d(\Delta v_i) \right) . \end{aligned} \tag{4.27}$$

Here n_0 denotes the foreign-gas number density at pressure P_0. [Eqs. (4.25) and (4.26) do not include the effect of collisions during t_{21} and t_{e3}.] Expressing the average change in z velocity magnitude as $\overline{|\Delta v_i|}$, we find in the limit of large t_{e3} when $k_e t_{e3}\overline{|\Delta v_i|} \gg 1$ that β' is expressed simply in terms of σ, the total VCC cross section, i.e.,

$$\beta'(k_e t_{e3}\overline{|\Delta v_i|} \gg 1) = 2(n_0/P_0)v_r t_{32}\sigma. \qquad (4.28)$$

Thus in the large-t_{e3} regime β' is independent of t_{e3} and σ can be determined directly. For shorter t_{e3}, Eq. (4.27) indicates that β' depends on t_{e3}. The details of this dependence are determined by the characteristics of the scattering kernel $f(\Delta v_i)$. Thus measurements of the t_{e3} dependence of β' can be used to infer the form of $f(\Delta v_i)$. These decay characteristics, which have already been demonstrated,[16] should prove quite useful in the study of VCC.

4. *Stimulated photon echo spectroscopy*

The recent discovery[16,37] that backward propagating echoes can be produced in gaseous samples as well as in solids[38,39] opens up exciting possibilities in spectroscopy. If the SP echo excitation pulses are narrow band (i.e., have pulse duration greater than inverse Doppler width), the forward and backward propagating pulses will only be resonant with the same atoms and hence produce an echo when their frequency is tuned to the center of the Doppler-broadened line. Using this fact, one can obtain Doppler-free spectra by monitoring the echo intensity as the frequency of the excitation laser is swept. This effect is similar to that observed in saturation spectroscopy[40]; however, instead of looking for a small decrease in probe attenuation at line center, in the case of counterpropagating echo spectroscopy there is no signal *except at line center.*

C. Sum-frequency trilevel echoes

The phase-mediated sum-frequency trilevel echo[2] (SF-I echo) is one of the most potentially useful new echo effects to be described here. It has already been applied to the study of foreign-gas-induced collisional relaxation of the $3S$-nS and $3S$-$nD_{3/2}$ superposition states of atomic sodium vapor.[1] Several foreign gases have been used and the principal quantum number n of the upper state has exceeded 40. The SF-I echo is produced in a nominally three-level atom of type a in Fig. 1. The sequence of excitation pulses necessary is shown in Fig. 6(a). In the simple case of three nondegenerate levels we find immediately from Eq. (1.32) that a memory term

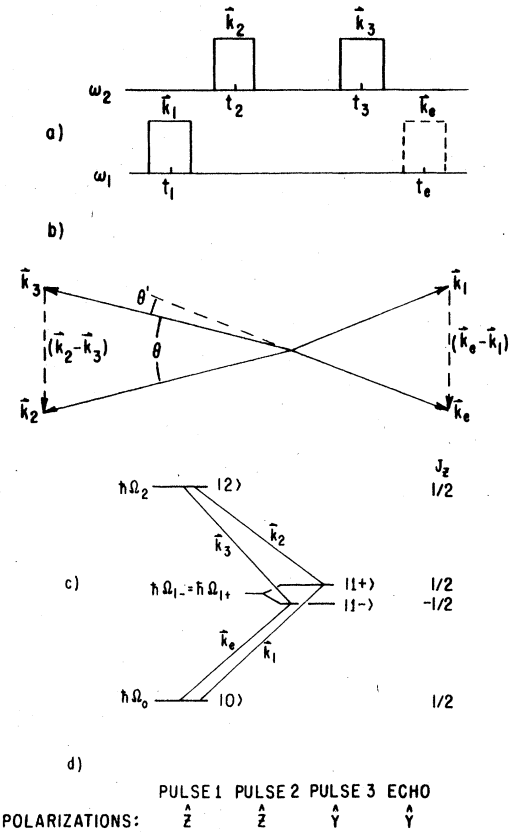

FIG. 6. (a) Frequencies and temporal sequence of the excitation pulses (solid lines) and the SF-I echo (dashed line) produced in type-a atoms. (b) Relative directions of the excitation pulses ($\vec{k}_1$, $\vec{k}_2$, $\vec{k}_3$) and the SF-I echo ($\vec{k}_e$) when the phase-matching condition is satisfied. (c) SF-I echo in a four-level atom. The $|1-\rangle$ and $|1+\rangle$ states are assumed to be degenerate magnetic sublevels of a single electronic state. The $|0\rangle$ and $|2\rangle$ levels are magnetic sublevels of two other distinct electronic levels. (d) Relative polarization of the excitation pulses and the echo when the SF-I echo is produced in the four-level atom of (c).

$$(T_\omega)_{10}^{\text{SF-I}} = \frac{iab\beta^* \sin\theta_1 \sin^2\tfrac{1}{2}\theta_2 \sin^2\tfrac{1}{2}\theta_3}{2|a||b||\beta|} \qquad (4.29)$$

appears in $(\rho_\omega)_{10}$ after the third pulse. Here the phase factors a, b, and β refer to the first, second, and third pulses, respectively. [In the limit θ_1, θ_2, $\theta_3 \ll 1$ Eq. (4.29) is identical with result obtained in Ref. 1.] From the definition of the phase factors for type a atoms, Eq. (1.13), we have

$$c_1\vec{\kappa}_1 = \vec{k}_1, \qquad (4.30a)$$

$$c_2\vec{\kappa}_2 = \vec{k}_2, \qquad (4.30b)$$

$$c_3\vec{\kappa}_3 = -\vec{k}_3, \qquad (4.30c)$$

where $\vec{k}_i$ is the wave vector of the ith excitation

pulse. From Eq. (4.30) it follows that the wave vector of the echo (if there is one) must satisfy the phase-matching condition [Eq. (2.6b)]

$$\vec{k}_e - \vec{k}_1 = \vec{k}_2 - \vec{k}_3 . \tag{4.31}$$

This is satisfied when the wave vectors are angled as shown in Fig. 6(b). It can also be satisfied with all pulses copropagating, but it is found that only the configuration of Fig. 6(b) leads to rephasing. Using Eqs. (2.8) and (2.9), we find that

$$t_e = \frac{\vec{k}_e \cdot \vec{D}}{k_e^2} = t_1 + \frac{\vec{k}_e \cdot \vec{k}_2}{k_e^2}(t_2 - t_1) - \frac{\vec{k}_e \cdot \vec{k}_3}{k_e^2}(t_3 - t_1) . \tag{4.32}$$

If θ and θ' of Fig. 6(b) are small, we may easily evaluate the scalar products to obtain

$$t_e = (k_2/k_1)(t_3 - t_2) , \tag{4.33}$$

where t_1 has been set equal to zero and we have used $k_2 = k_3$ and $k_1 = k_e$. Thus it can be seen that unless $k_2 > k_1 t_3/(t_3 - t_2)$ the atoms will not rephase to produce an echo.

We now calculate the degradation of the echo intensity as the angle θ is increased from 0. Using Eqs. (2.10) and (2.15), we find that

$$\vec{D}_\perp = \left[\vec{k}_2 + \vec{k}_e \frac{k_2}{k_e} \cos\left(\theta \frac{k_2 + k_1}{2k_1}\right)\right](t_2 - t_1) - \left[\vec{k}_3 + \vec{k}_e \frac{k_3}{k_e} \cos\left(\theta \frac{k_2 - k_1}{2k_1}\right)\right](t_3 - t_1) \tag{4.34}$$

and

$$|\vec{D}_\perp|^2 = \left(k_3 t_3 \frac{k_2 - k_1}{2k_1} - k_2 t_2 \frac{k_2 + k_1}{2k_1}\right)^2 \theta^2 , \tag{4.35}$$

where in Eq. (4.35) $t_1 = 0$ and it is assumed that θ, $\theta' \ll 1$. If $t_2 = 0$ it can be seen that $|D_\perp|^2$ above is smaller than in the case of photon or stimulated echoes by a factor of approximately $[(k_2 - k_1)/2k_1]^2$. This implies that if $k_1 \cong k_2$ the SF-I echo experiences only a relatively small reduction in intensity when the excitation beams are made noncollinear. Note also that when $\theta > 0$ the echo propagates in a direction removed from those of the excitation pulses. This makes SF-I echo detection quite simple especially when $k_1 \cong k_2$.

The SF-I echo is useful because of the relaxation measurements it makes possible. By observing the evolution of the density (or phase) matrix during the sequence of pulses it is found that the SF-I echo information is stored in the $|1\rangle$-$|0\rangle$ superposition state during t_{21} and t_{e3}, but during t_{32} it is stored in the $|2\rangle$-$|0\rangle$ two-photon superposition state. By monitoring foreign-gas-induced decay of the SF-I echo it is thus possible to determine the relaxation rate for the $|2\rangle$-$|0\rangle$ superposition. The details of such measurements are given in Ref. 1.

We have pointed out that when $k_1 \cong k_2$, making the excitation beams noncollinear facilitates observation of the echo. We now discuss a more general method of producing easily observable SF-I echoes. Consider the four-level system shown in Fig. 6(c). The degeneracy or near-degeneracy of the $|1\rangle$ level is essential to the effect described here. From left to right and top to bottom the elements of the 4×4 density matrix $\rho_\omega^{(4)}$ refer to the levels $|0\rangle$, $|1-\rangle$, $|1+\rangle$, and $|2\rangle$.

The three excitation pulses with phase factors a, b, and β which propagate along $\hat{x}$, $-\hat{x}$, and $-\hat{x}$, respectively, and have linear polarizations parallel to $\hat{z}$, $\hat{z}$, and $\hat{y}$, excite sequentially the $|1+\rangle$-$|0\rangle$, $|2\rangle$-$|1+\rangle$, and $|2\rangle$-$|1-\rangle$ transitions. The transformation matrix $M_R^{(4)}$, which determines the evolution of $\rho_\omega^{(4)}$ is obtained from the three-level M_R by simply noting that M_R represents a transformation performed on a "subspace" of the four-level system. Thus the three-level M_R is simply imbedded in a 4×4 identity matrix to form $M_R^{(4)}$. For example, for the first single-frequency excitation-pulse coupling levels $|1+\rangle$-$|0\rangle$

$$M_R^{(4)} = \begin{bmatrix} \cos\frac{1}{2}\theta_1 & 0 & \dfrac{-ia^* \sin\frac{1}{2}\theta_1}{|a|} & 0 \\ 0 & 1 & 0 & 0 \\ \dfrac{-ia \sin\frac{1}{2}\theta_1}{|a|} & 0 & \cos\frac{1}{2}\theta_1 & 0 \\ 0 & 0 & 0 & 1 \end{bmatrix} . \tag{4.36}$$

$M_R^{(4)-1}$ is obtained in the usual fashion by everywhere changing the sign of θ_1. By forming the $M_R^{(4)}$ matrices for the remaining two pulses and using the transformation equation Eq. (1.18) with an initial $\rho_\omega^{(4)}$ having population only in the $|0\rangle$ state, we find that after the three excitation pulses

$$\rho_\omega^{(4)} = \begin{bmatrix} \cos^2\frac{1}{2}\theta_1 & (-ia^*b^*\beta \sin\theta_1 \sin\frac{1}{2}\theta_2 \times \sin\frac{1}{2}\theta_3)/2|a||b||\beta| & \dfrac{ia^* \sin\theta_1 \cos\frac{1}{2}\theta_2}{2|a|} & (-a^*b^* \sin\theta_1 \sin\frac{1}{2}\theta_2 \times \cos\frac{1}{2}\theta_3)/2|a||b| \\ (iab\beta^* \sin\theta_1 \sin\frac{1}{2}\theta_2 \times \sin\frac{1}{2}\theta_3)/2|a||b||\beta| & \sin^2\frac{1}{2}\theta_1 \sin^2\frac{1}{2}\theta_2 \times \sin^2\frac{1}{2}\theta_3 & (-b\beta^* \sin^2\frac{1}{2}\theta_1 \sin\theta_2 \times \sin\frac{1}{2}\theta_3)/2|b||\beta| & (-i\beta^* \sin^2\frac{1}{2}\theta_1 \sin^2\frac{1}{2}\theta_2 \times \sin\theta_3)/2|\beta| \\ \dfrac{-ia \sin\theta_1 \cos\frac{1}{2}\theta_2}{2|a|} & (-b^*\beta \sin^2\frac{1}{2}\theta_1 \sin\theta_2 \times \sin\frac{1}{2}\theta_3)/2|b||\beta| & \sin^2\frac{1}{2}\theta_1 \cos^2\frac{1}{2}\theta_2 & (ib^* \sin^2\frac{1}{2}\theta_1 \sin\theta_2 \times \cos\frac{1}{2}\theta_3)/2|b| \\ (-ab \sin\theta_1 \sin\frac{1}{2}\theta_2 \times \cos\frac{1}{2}\theta_3)/2|a||b| & (i\beta \sin^2\frac{1}{2}\theta_1 \sin^2\frac{1}{2}\theta_2 \times \sin\theta_3)/2|\beta| & (-ib \sin^2\frac{1}{2}\theta_1 \sin\theta_2 \times \cos\frac{1}{2}\theta_3)/2|b| & \sin^2\frac{1}{2}\theta_1 \sin^2\frac{1}{2}\theta_2 \times \cos^2\frac{1}{2}\theta_3 \end{bmatrix} . \tag{4.37}$$

The important result is that $(\rho_\omega^{(4)})_{(1-)0}$ consists of a memory term identical to the one which produced the SF-I echoes in the nondegenerate three-level atom. Since the phase factors for the three- and four-level cases are identical, an echo with precisely the same characteristics as the SF-I echoes discussed earlier is produced on the $|1\rangle$-$|0\rangle$ transition. It will be noted Fig. 6(d) that the polarization of the echo is then normal to that of the only excitation pulse of the same frequency. This excitation pulse can be prevented from saturating the detector by a polarizer whose pass axis is aligned parallel to the echo polarization.[1] The second and third excitation pulses propagate in the direction opposite to the echo and hence do not make the detection of the echo difficult. For other types of trilevel echoes, for which there is often only one excitation pulse at the frequency of the echo, it is generally found that the echo-frequency excitation pulse can be eliminated by using the polarization technique described above. The other excitation pulses, regardless of their direction of propagation or polarization, can generally be eliminated by using appropriate bandpass filters or other frequency-selective detection. From these considerations it can be seen that the SF-I echo and other trilevel echoes can be observed without the use of troublesome optical shutters.

When performed in a four-level atom as described above, the SF-I echo still provides a measurement of the $|2\rangle$-$|0\rangle$ superposition decay rate. However, the intervals t_{21} and t_{e3} are no longer equivalent since the echo information is stored in nominally different superposition states.

D. Difference-frequency trilevel echoes

When a sample of type-b atoms [Fig. 1(b)] with the population initially in level $|0\rangle$ is excited with the sequence of three pulses shown in Fig. 7(a) a difference-frequency (DF) trilevel echo can be produced. Using the standard techniques to obtain the phase matrix after the third pulse, one finds that a memory term containing the phase factors $a^*b^*\alpha$ appears in $(\rho_\omega)_{12}$. The phase factors a, b, and α correspond to the first, second, and third excitation pulses, respectively. Using the definition of the phase factors in a type-b atom, Eq. (1.14), one finds that the $c_i\vec{\kappa}_i$ of Eq. (2.1) are given by

$$c_1\vec{\kappa}_1 = -\vec{k}_1\,, \tag{4.38a}$$

$$c_2\vec{\kappa}_2 = \vec{k}_2\,, \tag{4.38b}$$

$$c_3\vec{\kappa}_3 = \vec{k}_3\,. \tag{4.38c}$$

This immediately implies that the phase-matching

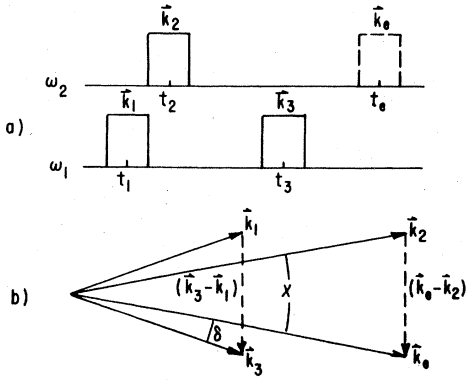

FIG. 7. (a) Frequencies and temporal sequence of excitation pulses (solid lines) and echo (dashed line) in the case of the DF echo in type-b atoms. (b) Phase-matched spatial orientations of the excitation pulses ($\vec{k}_1$, $\vec{k}_2$, $\vec{k}_3$) and the DF echo ($\vec{k}_e$).

condition [Eq. (2.6b)] is

$$\vec{k}_e = -\vec{k}_1 + \vec{k}_2 + \vec{k}_3\,. \tag{4.39}$$

A configuration of the wave vectors which satisfies this requirement and the rephasing requirement below is shown in Fig. 7(b). Using Eqs. (2.8) and (2.9), we find that the time of the echo is given by

$$t_e = t_1 + \frac{k_2}{k_e}(t_2 - t_1)\cos\chi + \frac{k_3}{k_e}(t_3 - t_1)\cos\delta\,, \tag{4.40}$$

where the angles χ and δ are defined in Fig. 7(b). For collinear excitation $t_e = t_2 + (k_3 t_3/k_e)$, where $t_1 = 0$ and $k_e = k_2$.

When $\chi > 0$ the degradation of the echo relative to $\chi = 0$ is found by using Eqs. (2.10) and (2.15), where

$$\vec{D}_\perp = (t_2 - t_1)\left(\vec{k}_2 - \vec{k}_e\frac{k_2}{k_e}\cos\chi\right) + (t_3 - t_1)\left(\vec{k}_3 - \vec{k}_e\frac{k_3}{k_e}\cos\delta\right). \tag{4.41}$$

Setting $t_1 = 0$ and assuming $\chi, \delta \ll 1$, we have

$$|\vec{D}_\perp|^2 \cong (t_3 k_3 \delta - t_2 k_2 \chi)^2\,. \tag{4.42}$$

It is apparent that for $t_2 > 0$ the echo intensity decreases rapidly with χ. If, however, $t_2 = 0$ and $k_1 \cong k_2$ the echo is relatively immune to the effects of making the excitation beams noncollinear.

Like the SF-I echo, the DF echo is potentially useful in that it allows measurements to be made of the relaxation properties of the $|2\rangle$-$|0\rangle$ superposition state. If $t_2 = 0$ the echo information is stored in the phase of the $|2\rangle$-$|0\rangle$ superposition at all times except between t_3 and t_e, when it is stored in the $|1\rangle$-$|2\rangle$ superposition state. As described in Ref. 1, relaxation during this interval can be compensated for by using excited-state

photon echoes, and the relaxation properties of the $|2\rangle$-$|0\rangle$ superposition determined. Like the SF-I echo, the DF echo can be detected by using the polarization technique.

E. Inverted-difference-frequency trilevel echo

If a sample of type-c atoms initially in state $|1\rangle$ is excited by any one of the pulse sequences shown in Fig. 8(a), 8(b), or 8(c), an echo may be produced. Any of these echoes, which we call inverted-difference-frequency (IDF) trilevel echoes, can be used to measure the relaxation characteristics of the $|2\rangle$-$|0\rangle$ superposition state. Between the second and third pulse in each of the excitation schemes shown the echo information is stored in the phase of the $|2\rangle$-$|0\rangle$ superposition state.

We give specific results only for the excitation scheme of Fig. 8(c). After the third excitation pulse $(\rho_\omega)_{01}$ contains a memory term with the phase factors $b^*a^*\beta$, where b, a, and β refer to the first, second, and third pulse, respectively. Using the definition Eq. (1.15) of the phase factors in a type-c atom, we find

$$c_1\vec{\kappa}_1 = -\vec{k}_1\,, \tag{4.43a}$$

$$c_2\vec{\kappa}_2 = \vec{k}_2\,, \tag{4.43b}$$

$$c_3\vec{\kappa}_3 = \vec{k}_3\,. \tag{4.43c}$$

Then using Eqs. (2.5) and (2.6b) we find that the phase-matching condition is

$$\vec{k}_e - \vec{k}_2 = \vec{k}_3 - \vec{k}_1\,. \tag{4.44}$$

A configuration of the wave vectors ($\vec{k}_i$ is the wave vector of the ith pulse) which satisfies Eq. (4.44) is shown in Fig. 8(d). Although a counter-propagating arrangement satisfies Eq. (4.44), it does not produce rephasing with $t_e > t_3$. The time of the echo, obtained from Eqs. (2.8) and (2.9), is found to be

$$t_e = t_1 + \frac{k_2}{k_e}(t_2 - t_1)\cos(\chi + 2\delta) + \frac{k_3}{k_e}(t_3 - t_1)\cos\delta\,, \tag{4.45}$$

where the angles χ and δ are defined in Fig. 8(d). The degradation of the echo with respect to the case $\chi = 0$ is determined by using Eqs. (2.10) and (2.15), where

$$\vec{D}_\perp = (t_2 - t_1)[\vec{k}_2 - \vec{k}_e(k_2/k_e)\cos(\chi + 2\delta)] + (t_3 - t_1)[k_3 - k_e(k_3/k_e)\cos\delta]\,, \tag{4.46}$$

and, with $t_1 = 0$ and $\chi, \delta \ll 1$,

$$|\vec{D}_\perp|^2 \cong [k_3 t_3 \delta + k_2 t_2(\chi + 2\delta)]^2\,. \tag{4.47}$$

Thus the degradation of the IDF echoes as χ increases from zero is similar to that of the DF echo. If $t_2 = 0$ and $k_1 \cong k_2$, making the excitation beams noncollinear degrades the echo only slightly. Since IDF echoes may be most useful in measuring the relaxation characteristics of superpositions between states such as the $3^2P_{1/2}$ and $3^2P_{3/2}$ states in sodium, it may often be true that $k_1 \cong k_2$ and echo detection can be facilitated by angling the excitation beams. Of course it is also possible to apply the polarization technique to detect the echo.

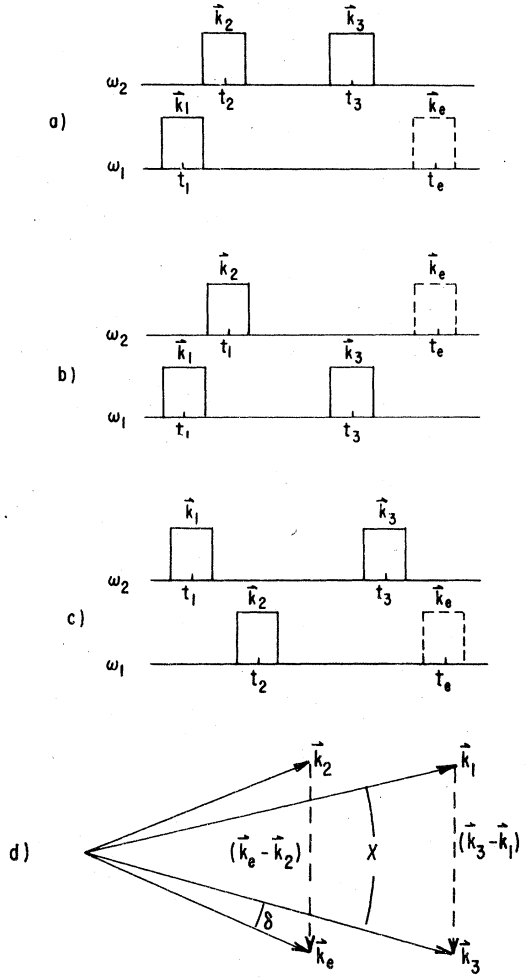

FIG. 8. (a)–(c) Various excitation-pulse (solid lines) schemes which produce IDF echoes in type-c atoms. (d) Phase-matched orientation of the excitation pulses and the IDF echo produced by the excitation pulses of (c).

ACKNOWLEDGMENT

This work was supported by the Joint Services Electronics Program (U. S. Army, U. S. Navy, and U. S. Air Force) under Contract No. DAAG29-77-C-0019, and by the Office of Naval Research under Contract No. N00014-78-C-0517.

[1]A. Flusberg, R. Kachru, T. Mossberg, and S. R. Hartmann, Phys. Rev. A 19, 1607 (1979).
[2]T. Mossberg, A. Flusberg, R. Kachru, and S. R. Hartmann, Phys. Rev. Lett. 39, 1523 (1977).
[3]E. L. Hahn, Phys. Rev. 80, 580 (1950); W. B. Mims, K. Nassau, and J. D. McGee, *ibid.* 123, 2059 (1961).
[4]I. D. Abella, N. A. Kurnit, and S. R. Hartmann, Phys. Rev. 141, 391 (1966).
[5]S. R. Hartmann, in *Proceedings of the International School of Physics "Enrico Fermi"* (Academic, New York, 1969), Vol. 42, p. 532.
[6]N. Kurnit, Ph.D. thesis, Columbia University, 1966 (unpublished).
[7]A. A. Maudsley, A. Wokaun, and R. R. Ernst, Chem. Phys. Lett. 55, 9 (1978); H. Hatanaka, T. Terao, and T. Hashi, J. Phys. Soc. Jpn. 39, 835 (1975).
[8]R. P. Feynman, F. L. Vernon, Jr., and R. W. Hellwarth, J. Appl. Phys. 28, 49 (1957).
[9]L. Allen and J. H. Eberly, *Optical Resonance and Two-Level Atoms* (Wiley, New York, 1975).
[10]D. Grischkowsky, M. M. T. Loy, and P. F. Liao, Phys. Rev. A 12, 2514 (1975).
[11]J. Ducuing, in Ref. 5, p. 421.
[12]E. Y. C. Lu and L. E. Wood, Phys. Lett. 44A, 68 (1973); M. Aihara and H. Inaba, Opt. Commun. 8, 280 (1973); J. Phys. A 6, 1709 (1973); 6, 1725 (1973); T. M. Makhviladze and L. A. Shelepin, Zh. Eksp. Teor. Fiz. 62, 2066 (1972) [Sov. Phys. JETP 35, 1080 (1972)].
[13]S. R. Hartmann, IEEE J. Quantum Electron. 4, 802 (1968).
[14]P. Hu, S. Geschwind, and T. M. Jedju, Phys. Rev. Lett. 37, 1357 (1976); 37, 1773 (1976).
[15]S. Aoki, Phys. Rev. A 14, 2258 (1976); A. Flusberg, T. Mossberg, R. Kachru, and S. R. Hartmann, Phys. Rev. Lett. 41, 305 (1978); H. Hatanaka and T. Hashi, J. Phys. Soc. Jpn. Lett. 39, 1139 (1975).
[16]T. Mossberg, A. Flusberg, R. Kachru, and S. R. Hartmann, Phys. Rev. Lett. 42, 1665 (1979).
[17]T. Baer and I. D. Abella, Phys. Lett. 59A, 371 (1976); Phys. Rev. A 16, 2093 (1977); A. Schenzle, S. Grossman, and R. G. Brewer, *ibid.* 13, 1891 (1976).
[18]A. I. Alekseev, Pis'ma Zh. Eksp. Teor. Fiz. 9, 472 (1969) [JETP Lett. 9, 285 (1969)]; A. I. Alekseev and I. V. Evseev, Zh. Eksp. Teor. Fiz. 57, 1735 (1969) [Sov. Phys. JETP 30, 938 (1970)].
[19]R. Weingarten, Ph. D. thesis, Columbia University, 1972 (unpublished); R. G. Brewer and E. L. Hahn, Phys. Rev. A 8, 464 (1973); 9, 1479 (1974); 11, 1641 (1975); A. Flusberg, Ph.D. thesis, Columbia University, 1975 (unpublished); M. Takatsuji, Phys. Rev. A 11, 619 (1975); A. Flusberg and S. R. Hartmann, *ibid.* 14, 813 (1976); M. Ducloy, J. Leite, and M. S. Feld, *ibid.* 17, 623 (1978).
[20]We note that certain echoes appear as the result of inhomogeneous dephasing which occurs during the excitation pulses; i.e., to account for them one must consider the atomic motion during the pulses. Such echoes were observed in Ref. 2 and explained in Ref. 1, where they were referred to as SF-II trilevel echoes. Echoes of this type are not directly covered by the analysis of this work but they may be treated with the techniques of this work by considering individual pulses to consist of a series of two or more subpulses. (See Appendix C of Ref. 1.)
[21]U. Fano, Rev. Mod. Phys. 29, 74 (1957).
[22]M. M. Salour and C. Cohen-Tannoudji, Phys. Rev. Lett. 38, 757 (1977); R. Teets, J. Eckstein, and T. W. Hänsch, *ibid.* 38, 760 (1977).
[23]The term "virtual echo" has been used in the past in a fashion similar to that in which we use it here [A. Saha and T. Das, *Theory and Applications of Nuclear Induction* (Saha Institute of Nuclear Physics, Calcutta, 1957)].
[24]D. S. Bethune, R. W. Smith, and Y. R. Shen, Phys. Rev. Lett. 37, 431 (1976); A. Flusberg, T. Mossberg, and S. R. Hartmann, *ibid.* 38, 59 (1977); *ibid.* 38, 694 (1977); M. Matsuoka, H. Nakatsuka, H. Uchiki, and M. Mitsunaga, *ibid.* 38, 894 (1977).
[25]A. Flusberg, T. Mossberg, and S. R. Hartmann, Opt. Commun. 24, 207 (1978).
[26]A. Compaan and I. D. Abella, Phys. Rev. Lett. 27, 23 (1971); R. Friedberg and S. R. Hartmann, Phys. Lett. 37A, 285 (1971); E. L. Hahn, N. S. Shiren, and S. L. McCall, *ibid.* 37A, 265 (1971).
[27]J. Schmidt, P. R. Berman, and R. G. Brewer, Phys. Rev. Lett. 31, 1103 (1973); P. R. Berman, J. M. Levy, and R. G. Brewer, Phys. Rev. A 11, 1668 (1975); I. V. Yevseyev and V. M. Yermachenko, Phys. Lett. 60A, 187 (1977); C. H. Wang, Phys. Rev. B 1, 156 (1970); T. Baer, Phys. Rev. A 18, 2570 (1978); A. I. Alekseev, I. V. Evseev, and V. M. Ermachenko, Zh. Eksp. Teor. Fiz. 73, 470 (1977) [Sov. Phys. JETP 46, 246 (1977)]; C. V. Heer, Phys. Rev. A 10, 2112 (1974); A. B. Doktorov and A. I. Burshtein, Zh. Eksp. Teor. Fiz. 63, 784 (1972) [Sov. Phys. JETP 36, 411 (1973)]; A. Flusberg, Opt. Commun. 29, 123 (1979); J.-L. LeGouët and P. R. Berman, Phys. Rev. A 20, 1105 (1979).
[28]P. R. Berman and W. E. Lamb, Jr., Phys. Rev. A 2, 2435 (1970); *ibid.* 4, 319 (1971); P. R. Berman, Phys. Lett. 43C, 101 (1978).
[29]C. K. N. Patel and R. E. Slusher, Phys. Rev. Lett. 20, 1087 (1968); T. Baer and I. D. Abella, Opt. Lett. 3, 170 (1978); B. Bölger and J. C. Diels, Phys. Lett. 28A, 401 (1968); R. G. Brewer and R. L. Shoemaker, Phys. Rev. Lett. 27, 631 (1971); R. G. Brewer and A. Z. Genack, *ibid.* 36, 959 (1976).
[30]M. Scully, M. J. Stephen, and D. C. Burnham, Phys. Rev. 171, 213 (1968); J. P. Gordon, C. H. Wang, C. K. N. Patel, R. E. Slusher, and W. J. Tomlinson, 179, 294 (1969); A. I. Alekseev and I. V. Evseev, Zh. Eksp. Teor. Fiz. 56, 2118 (1969) [Sov. Phys. JETP 29, 1139 (1969)]; 68, 456 (1975) [41, 222 (1975)]; T. M. Makhviladze and M. E. Sarychev, *ibid.* 69, 1594 (1975) [*ibid.* 42, 812 (1976)].
[31]P. Hu and H. M. Gibbs, J. Opt. Soc. Am. 68, 1630 (1978).
[32]We note that W. H. Hesselink and D. A. Wiersma [Chem. Phys. Lett. 56, 227 (1978)] working in solids have developed a useful technique for the detection of picosecond photon echoes.
[33]Certain of the characteristics of the stimulated echo as produced in three-level atoms were discussed by A. I. Siraziev and V. V. Samarthsev, in Opt. Spektrosk. 39, 730 (1975) [Opt. Spectrosc. 39, 413 (1975)].
[34]A. B. Doktorov and A. I. Burshtein (Ref. 27) provide a discussion of certain aspects of the behavior of stimulated echoes in the presence of velocity-changing collisions. They apparently did not realize that the stimulated echo could be used to study collisions af-

fecting atoms in a single state.
[35]B. L. Gyorffry, M. Borenstein, and W. E. Lamb, Jr., Phys. Rev. 169, 340 (1968); S. G. Rautian and I. I. Sobel'man, Sov. Phys. Usp. 9, 701 (1967); P. R. Berman, J. M. Levy, and R. G. Brewer, Phys. Rev. A 11, 1668 (1975).
[36]R. G. Breene, Rev. Mod. Phys. 29, 94 (1957).
[37]After this manuscript was in final form we received a preprint from M. Fujita, H. Nakatsuka, H. Nakanishi, and M. Matsuoka which also points out the possibility of the backward-propagating stimulated echo. [Phys. Rev. Lett. 42, 974 (1979)].
[38]N. S. Shiren, Appl. Phys. Lett. 33, 299 (1978).
[39]N. S. Shiren and T. G. Kazyaka, Phys. Rev. Lett. 28, 1304 (1972); E. I. Shtyrkov, V. S. Lobkov, and N. G. Yarmukhametov, Pis'ma Zh. Eksp. Teor. Fiz. 27, 685 (1978) [JETP Lett. 27, 648 (1978)].
[40]T. W. Hänsch, I. S. Shahin, and A. L. Schawlow, Phys. Rev. Lett. 27, 707 (1971).